HHS Public Access
Author manuscript
Circulation. Author manuscript; available in PMC 2022 December 07.

Published in final edited form as:
Circulation. 2021 December 07; 144(23): 1856–1875. doi:10.1161/CIRCULATIONAHA.121.055949.

CARMN is an Evolutionarily Conserved Smooth Muscle Cell-specific LncRNA that Maintains Contractile Phenotype by Binding Myocardin

Kunzhe Dong, Ph.D.[1,*], **Jian Shen, M.D.**[1,2,*], **Xiangqin He, Ph.D.**[1], **Guoqing Hu, D.D.S.**[1], **Liang Wang, M.D**[1,5], **Islam Osman, Ph.D.**[1], **Kristopher M. Bunting, M.D.**[1], **Rachael Dixon-Melvin, B.S.**[1], **Zeqi Zheng, M.D.**[5], **Hongbo Xin, Ph.D.**[3,4], **Meixiang Xiang, Ph.D.**[2], **Almira Vazdarjanova, Ph.D.**[1], **David J. R. Fulton, Ph.D.**[1,6], **Jiliang Zhou, Ph.D.**[1,#]

[1.]Department of Pharmacology and Toxicology, Medical College of Georgia, Augusta University, Augusta, Georgia, 30912, USA

[2.]Department of Cardiology, The Second Affiliated Hospital, Zhejiang University, Hangzhou, Zhejiang, 310009, China

[3.]The National Engineering Research Center for Bioengineering Drugs and the Technologies, Institute of Translational Medicine, Nanchang University, Nanchang, Jiangxi, 330031, China

[4.]School of Life Sciences, Nanchang University, Nanchang, Jiangxi, 330031, China

[5.]Department of Cardiology, The First Affiliated Hospital of Nanchang University, Nanchang, Jiangxi, 330006, China

[6.]Vascular Biology Center, Medical College of Georgia, Augusta University, Augusta, Georgia, 30912, USA

Abstract

Background: Vascular homeostasis is maintained by the differentiated phenotype of vascular smooth muscle cells (VSMCs). The landscape of protein coding genes comprising the transcriptome of differentiated VSMCs has been intensively investigated but many gaps remain including the emerging roles of non-coding genes.

Methods: We re-analyzed large-scale, publicly available bulk and scRNA-seq datasets from multiple tissues and cell types to identify VSMC-enriched lncRNAs. The *in vivo* expression pattern of a novel SMC expressed lncRNA, *Carmn* (CARdiac Mesoderm Enhancer-associated

[#]**Corresponding author: Jiliang Zhou, MD/PhD**, Department of Pharmacology & Toxicology, Medical College of Georgia, Augusta University, CB-3628 (Office); CB-3606 (Lab), 1459 Laney Walker Blvd, Augusta, GA 30912, Phone: 706-721-7582 (Office); 706-721-7583 (Lab), Fax: 706-721-2347, jizhou@augusta.edu.
[*]These authors contributed equally to this work.

DISCLOSURES
None

SUPPLEMENTAL MATERIAL
Supplemental Material and Methods
Supplemental Tables I–V
Supplemental Figures I–XI
Supplemental References: 3, 19, 26, 33, 35, 37–40, 42–49, 53, 59, 72, 76–97

Non-coding RNA) was investigated using a novel *Carmn* GFP knock-in reporter mouse model. Bioinformatics and qRT-PCR analysis were employed to assess *CARMN* expression changes during VSMC phenotypic modulation in human and murine vascular disease models. *In vitro,* functional assays were performed by knocking down *CARMN* with antisense oligonucleotides and over-expressing *Carmn* by adenovirus in human coronary artery SMCs. Carotid artery injury was performed in SMC-specific *Carmn* knockout mice to assess neointima formation and the therapeutic potential of reversing *CARMN* loss was tested in a rat carotid artery balloon injury model. The molecular mechanisms underlying *CARMN* function were investigated using RNA pull-down, RNA immunoprecipitation and luciferase reporter assays.

Results: We identified *CARMN*, which was initially annotated as the host gene of the *MIR143/145* cluster and recently reported to play a role in cardiac differentiation, as a highly abundant and conserved, SMC-specific lncRNA. Analysis of the *Carmn* GFP knock-in mouse model confirmed that *Carmn* is transiently expressed in embryonic cardiomyocytes and thereafter becomes restricted to SMCs. We also found that *Carmn* is transcribed independently of *Mir143/145*. *CARMN* expression is dramatically decreased by vascular disease in humans and murine models and regulates the contractile phenotype of VSMCs *in vitro*. *In vivo*, SMC-specific deletion of *Carmn* significantly exacerbated, while overexpression of *Carmn* markedly attenuated, injury-induced neointima formation in mouse and rat, respectively. Mechanistically, we found that *Carmn* physically binds to the key transcriptional cofactor myocardin, facilitating its activity and thereby maintaining the contractile phenotype of VSMCs.

Conclusions: *CARMN* is an evolutionarily conserved SMC-specific lncRNA with a previously unappreciated role in maintaining the contractile phenotype of VSMCs and is the first non-coding RNA discovered to interact with myocardin.

Keywords

Long non-coding RNA; *CARMN*; Smooth muscle cells; Vascular disease; Knock-in reporter

Subject Terms:

Smooth Muscle Proliferation and Differentiation; Vascular Biology; Vascular Disease

INTRODUCTION

Smooth muscle cells (SMCs) are the major contractile component of blood vessels and most hollow organs, such as bladder, intestine, and colon. Fully differentiated SMCs are characterized by the presence of a unique repertoire of contractile proteins.[1–8] In response to vascular injuries, VSMCs switch from a contractile to a synthetic phenotype, characterized by increased migration and proliferation as well as reduced expression of contractile pa SMC-specific lncRNA that promotes the controteins.[9] It has been reported that serum response factor (SRF), the transcription factor binding to CArG elements, plays a central role in regulating SMC phenotypes by interacting with a variety of cofactors.[10] As one of SRF-associated proteins, myocardin (MYOCD) is specifically expressed in cardiomyocytes and SMCs and is a potent activator of SM-specific genes.[11–13] However, the underlying molecular mechanism for regulation of SMC phenotypic switch and SRF-MYOCD interaction is not fully understood.

Although initially regarded as "junk DNA", >80% of human and mouse genomes is transcribed into a variety of classes of RNA.[14] For example, long non-coding RNAs (lncRNAs), defined as transcripts larger than 200 nucleotides and with no apparent protein-coding potential, outnumber all protein coding genes and have been shown to play critical roles in many physiological and pathological conditions.[15] Several lncRNAs have been implicated in SMC biology.[16–26] However, many of these lncRNAs are not conserved between species, not exclusively expressed in SMCs, and their expression has not been carefully tracked by *in vivo* reporter systems. These limitations collectively hinder our understanding of the importance of lncRNAs in SMCs and therefore a better exploration of lncRNA landscape in SMCs is required.

In this study, we used an *in silico* approach to probe unbiased proprietary and diverse publicly available bulk RNA-seq and scRNA-seq datasets to search for SMC-specific lncRNAs. This search identified *CARMN* (CARdiac Mesoderm Enhancer-associated Non-coding RNA) as a highly abundant, highly conserved SMC-specific lncRNA. *CARMN* was recently reported to play roles in cardiac differentiation,[27, 28] and was initially annotated as a host lncRNA for the *MIR143/145* cluster, the best characterized microRNAs in regulating SMC differentiation and phenotypic modulation.[29–34] In this study, we confirmed the expression specificity of *Carmn* using a novel GFP knock-in (KI) reporter mouse model and discovered that *CARMN* is down-regulated in various vascular diseases. We further found that *Carmn* is critical for maintaining VSMC contractile phenotype both *in vitro* and *in vivo* by directly binding to MYOCD and potentiating MYOCD function. These findings collectively suggest that *CARMN* is a key regulator of VSMC phenotype and represents a potential therapeutic target for treatment of SMC-related proliferative diseases.

METHODS

Detailed methods are provided in the Supplemental Material. The data, analytic methods including R scripts used for analyzing transcriptome datasets, and related materials will be made available from the corresponding author upon reasonable request. The amended mouse *Carmn* V2 and V3 cDNA sequences have been deposited into GenBank under accession number MN904529 and MN904530, respectively. Bulk RNA-seq, scRNA-seq, ChIP-seq and ATAC-seq datasets used in this study are fully described in the Supplemental Methods. All animal studies have been approved by the Institutional Animal Care and Use Committee of Augusta University and conducted in accordance with the National Institutes of Health Guide for the Care and Use of Laboratory Animals. There are no human subjects in this study.

Statistical Analysis

GraphPad Prism (Version 9.2.0) was used for the statistical analysis. All data are expressed as mean ± SEM of at least three independent experiments. Tests used for statistical significance evaluations are specified in figure legends. An unpaired two tailed *t*-test was used for data involving two groups only. Two-way analysis of variance (ANOVA) or two-way repeated measures ANOVA followed by a Bonferroni correction was used for data involving more than two groups. Values of $P \leq 0.05$ were considered statistically significant, except for analysis of bulk RNA-seq, scRNA-seq, microarray and ATAC-seq data which used FDR (false discovery rate)-adjusted $P < 0.05$ as the threshold for statistical significance.

RESULTS

CARMN is a highly abundant SMC-specific lncRNA in human

To identify SMC-enriched lncRNAs in human, we analyzed 2 independent bulk RNA-seq datasets generated from different human cell types. This unbiased analysis revealed *CARMN* is the only VSMC-enriched lncRNA identified from both datasets (Figure 1A and B, Table I in the Supplement). Furthermore, *CARMN* locus in human VSMCs is enriched with active histone mark H3K27ac and lacks repressive mark H3K27me3, in contrast to human umbilical vein endothelial cells (Figure 1C). Examination of two additional promoter-related histone modifications, H3K4me2 and H3K4me3, identified two potentially independent promoters upstream of *MIR143/145* and *CARMN* in SMCs (Figure I A in the Supplement). *CARMN* is mostly expressed in vascular tissues, followed by SMC-enriched gastrointestinal (GI) tissues as revealed by GTEx database (Figure 1D). Strikingly, *CARMN* is consistently within the top 15 most abundant lncRNAs expressed in different human arteries and is the most abundant lncRNA among those with features of evolutionary conservation and artery-specific expression pattern. In contrast, the other previously reported lncRNAs such as *MALAT1* and *NEAT1* lack specific expression for SMC lineages, or are low level non-conserved lncRNAs (Figure 1E).[16–24, 26] Re-analyzing a scRNA-seq dataset generated from coronary arteries of four human cardiac transplant recipients (GSE131778) [35] suggested *CARMN* expression is enriched in SMCs and pericytes which also express many SMC markers,[36] and is sporadically distributed in some fibroblast cells (Figure 1F and Figure I B–C in the Supplement). The expression pattern of *CARMN* is consistent with the known SM-specific markers such as *MYH11*, *ACTA2, CNN1* and *TAGLN* (Figure 1F and Figure I D in the Supplement). This analysis also revealed that *CARMN* was down-regulated in phenotypically modulated SMCs compared to normal VSMCs (Figure 1F). Taken together, these unbiased large-scale bioinformatics analyses demonstrate that *CARMN* is an abundantly and specifically expressed lncRNA in SMCs and in SM-enriched tissues in human.

Carmn is a highly conserved SMC-specific lncRNA in mouse

To identify lncRNAs enriched in mouse aorta, we re-analyzed bulk RNA-seq of adult mouse aortic tissues [37] and 5 other non-SM tissues.[38] This analysis revealed that *Carmn* is the most abundant aorta-enriched lncRNA (Figure 2A) and stands out from previously reported SMC-related lncRNAs [16, 18, 21, 22, 24–26] as having high abundance, evolutionary conservation, and a tissue-specific expression pattern in mouse aorta (Figure 2B). Subsequent qRT-PCR analysis validated the preferential expression of *Carmn* in thoracic aorta in mice (Figure 2C). Analysis of scRNA-seq data of normal adult mouse thoracic aorta [39] showed that *Carmn* is selectively expressed in aortic SMCs (Figure 2D and Figure II A–B in the

Supplement), which is further confirmed by an independent scRNA-seq dataset of mouse aorta (GSE117963) (Figure II C–E in the Supplement).[40]

RACE (Rapid Amplification of cDNA Ends) assay using adult mouse aorta cDNA failed to detect the isoform V1 annotated in UCSC database that encompasses *Mir143* and *Mir145*, while revealed the presence of amended V2 and V3 transcripts (Figure 2E, **top panel**). Our V2 (1228 bp) transcript had an extended exon 4 (GenBank accession number: MN904529), and V3 (759 bp) had a shorter exon 3 (GenBank accession number: MN904530) relative to annotated versions. None of them contain *Mir143* or *Mir145* (Figure 2E, **middle panel**). Consistently, bulk RNA-seq of mouse aorta [37] revealed splicing junctions covering V2 and V3, but not exon 4 and exon 5 that are unique to the annotated transcript V1 (Figure 2E, **bottom panel**). qRT-PCR data using primers specifically targeting different isoforms (Figure II F in the Supplement) suggested that V2 transcript is the most abundant one in mouse aorta (Figure 2F).

In silico prediction and *in vitro* transcription and translation assay demonstrated that the novel transcripts V2 and V3 are bona fide lncRNA (Figure II G in the Supplement and Figure 2G). Interestingly, a homologous lncRNA of *Carmn* is present in pig (*LOC100514340*) that is independently annotated from *MIR143/145* (Figure II H in the Supplement). Furthermore, examination of zebrafish genome (*ENSDART00000194758*) shows a predicted transcript of *Carmn* based on expressed sequence tag (EST) distancing from the microRNA cluster (Figure II I in the Supplement). Although there is no *Carmn* gene annotated in rat genome, we cloned a portion of rat *Carmn* cDNA sequence that is positionally conserved *to Mir143/145* by using primers located within the homologous region of mouse (Figure 2H and I). Taken together, we discovered that *Carmn* is a highly conserved SMC-specific lncRNA and validated it is transcribed independently of *Mir143/145* cluster at least in mouse aorta.

GFP KI reporter mouse model confirms the SMC-specific expression of *Carmn in vivo*

To visualize the expression of *Carmn in vivo*, we generated a KI mouse model by insertion with a promoterless, reversed splicing acceptor (SA)-membrane bound GFP gene trap cassette, which is flanked by two pairs of oppositely orientated *Lox2272* sites [41] and *LoxP* sites into intron 2 (referred to as conditional, PFG) (Figure 3A). Upon Cre-mediated deletion of exon 2 and inversion of the reversed GFP cassette (PFG to GFP), the inserted SA will prematurely terminate *Carmn* expression by splicing of exon 1 to the GFP cassette, while turning on GFP expression under control of the endogenous *Carmn* promoter (referred to as GFP). GFP expression should therefore faithfully display the endogenous *Carmn* expression *in vivo* while at the same time disrupting *Carmn* expression. We first crossed the female *Carmn*$^{PFG/WT}$ (PW) mice with male mice expressing ubiquitous *CMV-Cre* to invert the GFP cassette in all mouse tissues (Figure 3B). Genotyping results confirmed Cre-mediated recombination within the *Carmn* locus only in the GW heterozygous mouse (Figure 3C). Western blotting indicated GFP expression is restricted to the aorta, while absent in heart, skeletal muscle and brain of GW heterozygous mice (Figure 3D). Consistently, direct visualization of GFP fluorescence revealed specific expression in aorta and coronary arteries (Figure 3E), as well as in other hollow organs such as bladder, gallbladder, intestine, and stomach, and in regions of SMCs in brain and quadriceps muscles, bronchus of lung, skeletal muscle of GW heterozygous mice (Figure III in the Supplement). Data from co-immunostaining demonstrated that GFP is colocalized with SMC marker ACTA2 in medial layer, but not in endothelial or adventitia cells of GW mouse aorta (Figure 3F). RNA FISH (Fluorescent *in situ* hybridization) assays further revealed that *Carmn* expression is exclusively confined to SMC nuclei of mouse aorta (Figure 3G) and cultured mouse VSMCs transduced with *Carmn* adenovirus (Figure 3H). Collectively, these results provide direct *in vivo* evidences showing that *Carmn* is specifically expressed in the nuclei of SMCs.

Carmn is transiently expressed in cardiomyocytes during embryogenesis

Because *CARMN* was previously reported to play roles in regulating cardiac specification,[27, 28] we hypothesized that it may be transiently expressed in cardiomyocytes during development. Re-analysis of public scRNA-seq datasets showed that *Carmn* expression is present in 8.6% of cardiomyocytes at E10.5 [42] (Figure IV A in the Supplement) and is absent in cardiomyocytes but confined to SMCs/pericytes in adult mouse heart (Figure IV B in the Supplement).[43, 44] Further IF staining analysis for GFP on sections of GW embryos revealed that *Carmn* expression is primarily co-localized with SMC/early cardiac marker ACTA2 in dorsal aorta or left carotid artery while slightly overlapped with cardiac marker TNNT2 in both left and right ventricles at E11.5 and E13.5 (Figure IV C–F in the Supplement). The percentage of cardiomyocytes expressing *Carmn* is slightly higher in left ventricle than that in right ventricle and exhibits a declining trend with embryonic development from E11.5 (7.1% in left ventricle and 4.9% in right ventricle) to E13.5 (4.7% in left ventricle and 3.8% in right ventricle) in both ventricles (Figure IV C–F). Strikingly, at E16.5, *Carmn* expression is restricted to SMCs of carotid artery or in the arteriolar SMCs of the heart, but not in endothelium or cardiomyocytes (Figure 3I and Figure IV G in the Supplement). Similarly, *CARMN* expression is observed to some extent in cardiomyocytes in human developmental 6.5–7 post conception weeks heart (Figure V A in the Supplement),[45] while restricted to SMCs and pericytes in adult human heart (Figure V B in the Supplement).[46] Taken together, these results suggest that *CARMN* is transiently expressed in cardiomyocytes during early embryonic development but becomes confined to SMCs as development progresses in both mouse and human.

CARMN is downregulated in vascular diseases

Quantification analysis of scRNA-seq data of human diseased coronary artery (Figure 1F) showed that both the percentage of *CARMN* positive cells and *CARMN* expression level are lower in modulated SMCs compared to normal SMCs (Figure 4A and B). Targeted re-analysis of published transcriptomic datasets revealed that *CARMN* is significantly down-regulated in human atherosclerotic arteries and cerebral arteries with aneurysms (Figure 4C and D).[47, 48] Although not statistically significant, the intensity of multiple ATAC-seq peaks that represent chromatin accessibility of the *CARMN* gene locus, similar to the *MYH11* gene, is remarkably decreased in human atherosclerotic coronary arteries compared to normal coronary arteries (Figure 4E and Figure VI A–C in the Supplement).[49] To extend these findings to rodent vascular disease models, we re-analyzed scRNA-seq data (GSE131776) of ascending aorta from *Myh11*-CreER^{T2} lineage tracing mice on the *ApoE*$^{-/-}$ background at multiple time points, including baseline before a high-fat diet

(HFD), as well as after 8 and 16 weeks of HFD feeding.[35] This analysis revealed the majority of cells expressing *Carmn* (>80%) are derived from lineage traced SMCs (Figure 4F and Figure VII A–C in the Supplement) and confirmed *Carmn* is predominantly expressed in SMCs and pericytes while minimally expressed in fibroblast cells (Figure 4F and Figure VII D in the Supplement). Compared to normal SMCs, phenotypically modulated SMCs exhibit a marked reduction in the percentage of *Carmn* positive cells and *Carmn* expression levels over the course of disease progression that reaches statistical significance at 16 weeks after HFD (Figure 4G), which parallels the SM marker *Myh11* but is opposite to the *Ly6a* (aka Sca-1) that has been reported to be up-regulated during SMC phenotypic switching [35, 40] (Figure VII E in the Supplement). About 4.6% of modulated SMCs are SMC-lineage negative (Figure VII F in the Supplement), which likely reflects cells originating from non-SMCs such as adventitia/media progenitor cells and endothelial cells which undergo myogenic differentiation to become SMC-like cells during atherogenesis.[50, 51] The percentage of *Carmn* positive cells and *Carmn* expression levels are statistically lower in both SMC lineage positive and negative cells as compared to normal contractile SMCs at 16 weeks after HFD (Figure VII G in the Supplement), suggesting that *Carmn* is down-regulated in phenotypically modulated SMCs, regardless of their origin. It has been reported that a rare population of medial MYH11 positive SMCs expresses *Ly6a* and progressively downregulates contractile SMC genes and upregulates genes associated with SMC responses to inflammation and growth factors.[40] Consistently, our scRNA-seq analysis revealed that some normal SMCs express *Ly6a* (Figure VII E in the Supplement) and some of these medial $Myh11^{+}/Ly6a^{+}$ cells express *Carmn* (Figure VII E and H in the Supplement), which accounts for 0.05% of the total MYH11 positive contractile SMCs at baseline with an increase to 0.75% at 16 weeks after HFD (Figure VII H in the Supplement). Since it has been postulated that medial *Ly6a* positive SMCs can contribute to atherosclerotic lesion cells,[40, 52] it will be interesting to investigate whether *Carmn* regulates this process in the future. The enrichment of *Carmn* in SMCs and downregulation in modulated SMCs (statistically significant at 16 and 26 weeks after HFD) was further confirmed in an additional scRNA-seq dataset of lineage-traced aortic SMCs from the atherosclerotic *Ldlr* KO mouse model (GSE155513) (Figure VIII in the Supplement). [53] In an additional, independent scRNA-seq dataset of lineage-traced mouse aortic SMCs (GSE117963), a remarkable decrease in *Carmn* expression was observed in phenotypically modulated SMCs at 18 weeks after HFD feeding although it was not statistically signficant (Figure IX in the Supplement). [40] The decrease of *Carmn* expression in mouse atherosclerotic aortic tissues was independently validated by qRT-PCR (Figure 4H). Additional RNA-seq and qRT-PCR analyses indicated that *CARMN* expression is decreased in balloon-injured carotid arteries in rat (Figure 4I), human saphenous vein SMCs (HSVSMCs) stimulated with PDGF-BB or IL-1α (Figure 4J),[19, 54] HCASMCs induced by switching the culture medium from a differentiation to a growth medium (Figure 4K), and rat vascular SMCs treated with PDGF-BB (Figure 4L and M). Collectively, these data suggest *CARMN* expression is decreased during VSMC phenotypic modulation in human diseased artery, in rodent models of vascular wall diseases and in cultured VSMCs in response to growth and inflammatory stimuli.

CARMN promotes VSMC contractile phenotype *in vitro*

To determine the causality of *CARMN* down-regulation *in vitro*, we knocked down endogenous *CARMN* with phosphorothioate modified antisense oligonucleotide (ASO) in HCASMCs. Knocking down *CARMN* significantly enhanced cell proliferation (Figure 5A and B) and migration (Figure 5C), while attenuated the expression of SM-contractile proteins at both mRNA and protein levels (Figure 5D–F), as well as *MIR145* expression. *MIR143* expression was slightly but not significantly reduced (Figure 5D). Conversely, over-expression of *CARMN* promoted a contractile phenotype as indicated by increased numbers of spindle shaped HCASMCs (Figure 5G and H), decreased VSMC proliferation and migration (Figure 5I–K), and enhanced expression of SM-contractile genes at both mRNA and protein levels, as well as both *MIR143* and *MIR145* expression (Figure 5L–N). To assess functional roles of *Carmn* on individual cells, we performed IF staining for MYH11 in HCASMCs transduced with GFP or *Carmn* adenovirus and randomly selected 50 cells from each group to quantify IF signal intensity. Positive staining for MYH11 confirmed the SMC identity of these cells and demonstrated that *Carmn* over-expression generally increases MYH11 abundance in individual cells (Figure X in the Supplement). Collectively, these results suggest that *CARMN* is critical in maintaining a contractile phenotype of VSMCs *in vitro*.

SMC-specific deletion of *CARMN* exacerbates neointima formation in mice

To investigate a functional role of *Carmn* in SMCs *in vivo*, we generated SM-specific *Carmn* inducible KO (iKO) mice by crossing *Carmn* KI mice (PFG mice) with *Myh11*-CreER^{T2} mice (Figure 6A). SM lineage tracing mice (*Carmn*$^{W/W}$; *Myh11*-CreER^{T2}; mTmG$^{+/-}$) that express GFP specifically in SMCs upon tamoxifen-induced Cre recombinase activation, served as control mice to exclude potential cytotoxicity caused by the expression of GFP or Cre in SMCs of *Carmn* iKO mice (Figure 6B). In adult mice, tamoxifen was injected (10x) to initiate Cre activation and 2 weeks later, vascular injury was induced with left carotid artery (LCA) ligation. Neointima formation was assessed 14 days after injury (Figure 6C). Specific deletion of *Carmn* in the arteries of SM-specific *Carmn* iKO mice was validated by detection of the GFP allele (Figure 6D). qRT-PCR analysis further demonstrated SM-specific *Carmn* deletion leads to complete loss of *Carmn* expression and significant down-regulation of SM contractile genes including *Mylk* and *Acta2* in thoracic aorta (Figure 6E). Direct visualization of GFP in control right carotid arteries (RCA) revealed that GFP expression is restricted to the medial layer of RCAs in both groups (Figure 6F). In the injured LCA of SM lineage tracing control mice, the GFP signal was comparable between the neointima and medial layer, as GFP labels SMCs-derived cells prior to injury and independent of their altered phenotypes.[55] However, in *Carmn* iKO mice, GFP signal that represents endogenous *Carmn* expression was dramatically decreased in the neointima as compared to medial layer (Figure 6F), supporting our observations that *Carmn* expression is decreased in phenotypically modulated SMCs (Figure 4). HE staining further showed that the formation of neointima in injured LCA of *Carmn* iKO mice is markedly exacerbated versus control mice (Figure 6G and H). Furthermore, co-staining of ACTA2 and MKI67 revealed that *Carmn* deletion in SMCs significantly increases the total number of MKI67-postive proliferating VSMCs in injured LCA (Figure 6I and J). These data suggest that loss of *Carmn* expression in SMCs exacerbates neointima formation due to increased VSMC proliferation.

Restoration of *Carmn* expression attenuates neointima formation and SM dedifferentiation in rats

We next sought to test whether restoration of *Carmn* expression is capable of reversing VSMC phenotypic change *in vivo*. We transduced *Carmn* adenovirus in rat LCA immediately following balloon injury. Injured LCA infected with GFP virus served as control, in addition to the contralateral control of the intact RCA. Arteries were then harvested 14 days post injury for analyzing neointima size and SM-specific gene expression (Figure 7A). qRT-PCR first confirmed that endogenous *Carmn* expression is significantly down-regulated in GFP-infused injured LCA compared to control RCA, while local delivery of *Carmn* adenovirus dramatically restored the expression of *Carmn* (Figure 7B). Histological analysis revealed over-expression of *Carmn* significantly attenuates injury-induced neointima formation as indicated by decreased neointima/media layer area ratio (Figure 7C and D). IF staining of proliferation marker MKI67 and SM marker MYH11 further demonstrated that restoration of *Carmn* expression inhibits VSMC proliferation while alleviating injury-induced downregulation of MYH11 (Figure 7E and F). Moreover, over-expression of *Carmn* partially, but significantly, inhibited injury-induced downregulation of SM-specific genes at both mRNA (Figure 7G) and protein levels (Figure 7H and I). Taken together, these data demonstrate that lncRNA *CARMN* plays a critical role in promoting VSMC contractile phenotype *in vivo*.

CARMN directly binds to MYOCD to potentiate MYOCD function

The observations that *CARMN* is a nuclear-restricted lncRNA and over-expression of exogenous *Carmn* by adenoviral system is functional (Figure 5 and Figure 7), a mechanism that is not observed for *cis*-acting lncRNAs,[56, 57] indicate a potential *trans* mechanism of action of *Carmn*. We performed an *in silico* prediction and identified 55 putative *Carmn*-interacted proteins (Table V in the Supplement). *MYOCD* and *SRF*, two most potent mediators of SMC differentiation,[10, 12] were captured (Figure 8A) and their potential interaction with *Carmn* was further supported by an additional prediction tool RPIseq (Figure XI A in the Supplement).[58] *In vitro* RNA immunoprecipitation (RIP) assays demonstrated that *Carmn* was specifically precipitated by MYOCD instead of SRF (Figure 8B). MYOCD and *Carmn* interaction was further confirmed by *in vivo* RIP using anti-MYC antibody to immunoprecipitate aortic lysates extracted from MYC/HA-tagged *Myocd* mouse (Figure 8C and Figure XI B in the Supplement).[59] In a complementary approach, biotin-labeled *in vitro* transcribed *Carmn* sense transcript, but not antisense transcript, directly pulled down MYOCD, rather than SRF (Figure 8D). *Carmn* retrieved SRF only in the presence of MYOCD, which is attributed to the known physical interaction of MYOCD and SRF,[12] instead of direct *Carmn*/SRF binding (Figure 8D). Further RNA pull-down assays using a series of truncated MYOCD mutants [60] (Figure XI C in the Supplement) suggested that *Carmn* specifically interacts with MYOCD at the regions containing the basic (++), glutamine-rich (Q) and SAP domains where SRF binds (Figure 8E and Figure XI C in the Supplement).

We next tested the functional consequence of the physical interaction between *Carmn* and MYOCD. Data from reporter assays demonstrated that *Carmn* alone has no effect on the basal activity of SM-specific gene promoters but significantly promotes MYOCD-induced transactivation activity in a CArG-dependent manner (Figure 8F). Consistently, over-expressing *Carmn* significantly enhanced MYOCD-activated expression of SM-specific gene CNN1 in 10T1/2 cells at both mRNA and protein levels. Expression of several additional SM markers such as *Myh11* and *Acta2*, although not statistically significant, exhibited a trend towards an increase following MYOCD over-expression in the presence *Carmn* (Figure 8G–I). Furthermore, inactivation of endogenous *Carmn* mediated by Cre adenovirus in VSMCs isolated from *Carmn*$^{PFG/PFG}$ mice significantly abrogated MYOCD-induced SM-specific gene expression at both mRNA and protein levels (Figure 8J–L, Figure XI D in the Supplement). Interestingly, deletion of *Carmn* or overexpression of *Myocd* had no effect on the expression of non-CArG-dependent SM-specific genes such as *Notch3*, *Apeg* and *Eln* (Figure XI E in the Supplement). Furthermore, over-expression of *MIR143/145* was unable to rescue the *Carmn* deficiency-induced down-regulation of SM markers including *Myh11* and *Mylk* in mouse VSMCs (Figure XI F in the Supplement). Together, these mechanistic results suggest that *Carmn* is critical for VSMC differentiation by directly binding and potentiating MYOCD function *in trans*, but independent of *MIR143/145*.

In summary, our study demonstrates a previously unappreciated role of the nuclear lncRNA *CARMN* in maintaining the contractile phenotype of VSMCs in healthy artery by directly binding to MYOCD, thereby potentiating MYOCD function *in trans* (Figure 8M, top panel). *CARMN* also mediates the expression of its neighboring gene *MIR143/145* cluster in VSMCs through an unclear mechanism. Conversely, in diseased arteries, expression of *CARMN* is down-regulated, thereby attenuating the transactivation activity of MYOCD/SRF complex on SMC-specific gene expression and triggering dedifferentiation of VSMCs, leading to exacerbated neointima formation (Figure 8M, bottom panel).

DISCUSSION

Distinct from lncRNAs previously implicated in SM biology,[16–26] we identified *CARMN* as a highly abundant and conserved SMC-enriched lncRNA through a series of *in silico* analysis. Using a novel GFP KI reporter mouse model, we demonstrate that *Carmn* is transiently expressed in embryonic cardiomyocytes and thereafter becomes restricted to adult SMCs *in vivo*. Future investigations are necessary to unveil the mechanisms underlying the transcriptional regulation of the SMC-specific expression of *CARMN*. Additionally, *Carmn* expression is occasionally observed at low levels in fibroblasts. It will be of interest to test potential functional roles of *Carmn* in fibroblasts, especially in *Ly6a* positive fibroblast cells in future studies.

Our study reveals that *CARMN* expression is markedly reduced in the diseased vascular wall of humans and rodent vascular disease models, and in VSMCs in response to stimuli of phenotypic modulation *in vitro*. In agreement with the previous studies showing that *CARMN* depletion is associated with decreased SMC-specific genes during CPC specification [27, 28] and in HCASMCs,[61, 62] data from gain- and loss-of-function assays demonstrate that *CARMN* is sufficient and required to promote the contractile phenotype of VSMCs *in vitro*. Moreover, SM-specific deletion of *Carmn* in mice markedly exacerbates injury-induced neointima formation while restoration of *Carmn* expression in rats attenuates balloon injury-induced vascular remodeling. In a rat artery injury model, we observed that in contrast to the dramatic inhibition of neointima formation, *Carmn* over-expression only partially restored injury-induced loss expression of SMC contractile genes. This suggests that *Carmn*-mediated inhibition of SMC proliferation and migration also play a critical role in attenuating intimal thickening, in addition to enhancing the expression of SMC contractile genes. Furthermore, it has been shown that non-SMCs such as adventitial and medial progenitor cells may be additional contributors to neointima formation following injury.[50, 51, 63–67] We cannot rule out the possibility that ectopic expression of *Carmn* in non-SMCs may also play a role in repressing neointima formation, which is also a limitation of two recent studies using *Carmn* global KO mice [61] or gapmeR-mediated *Carmn* knockdown mice [62]. To address this, we generated a SM-specific *Carmn* iKO mouse model and we now provide direct evidence for a functional role of *Carmn* in SMCs *in vivo*. Collectively, these findings suggest that increasing or maintaining expression of *CARMN* represents a potentially promising strategy for the treatment and prevention of VSMC-related proliferative diseases.

CARMN was initially known as the host gene for the *MIR143/145* cluster, that are derived from a common precursor and have been reported to be highly enriched in SMCs and important for regulation of SMC phenotypic modulation.[29–32, 34, 68] Our results provide several additional lines of evidence supporting the previous reports that *CARMN* is transcribed and functionally independent of *MIR143/145* in fetal [27] and adult CPCs,[28] and in HCASMCs.[61, 62] First, distinct promoter-associated H3K4me2 and H3K4me3 marks that are known to be enriched at the transcription start site,[69] exist immediately upstream of both *CARMN* and *MIR143/145* in human VSMCs. Second, all *Carmn* isoforms do not overlapped with *Mir143/145* in mouse aorta and in other species like pig. Finally, the *Carmn* transcript V2 used for adenovirus construction does not contain *Mir143/145* but is sufficient to promote contractile phenotype of human VSMCs and to rescue the injured-induced neointima hyperplasia and SMC dedifferentiation *in vivo*.

As a neighboring gene of *CARMN*, we observed that *MIR143/145* expression is induced by over-expression of *Carmn* in human VSMCs while it is inhibited in mouse aortic SMCs with *Carmn* deletion. Like other SM markers, *MIR143/145* expression is enriched in contractile SMCs in a MYOCD/SRF complex-dependent manner and is down-regulated in phenotypically modulated SMCs.[32] Therefore, it is difficult to distinguish whether the expression oscillation of *MIR143/145* in SMCs following *CARMN* expression change is through *in cis* function of *CARMN*, or due to secondary effect of *CARMN*-mediated SMC phenotypic switching. Some lncRNAs are reported to act both *in cis* and *in trans*.[70] *CARMN* may represent one example of a lncRNA using both mechanisms since *CARMN* is an enhancer-expressed lncRNA which has been reported to act *in cis*.[57] It has been reported that *MIR143/145* cluster is a key player in promoting SMC differentiation through diverse mechanisms such as directly inhibiting transcription factors that suppress MYOCD, including KLF4, KLF5 and ELK1.[32] However, our over-expression assay showed that *MIR143/145* has no effect on SM-specific gene expression in control VSMCs, despite the dramatic decrease in *Klf4* and *Klf5* expression. The reason for the discrepancy is unclear and remains to be determined. In addition, we found restoration of *MIR143/145* in *Carmn*-null VSMCs slightly but not significantly up-regulates the expression of *Myh11* and *Mylk*, suggesting that *CARMN*-mediated *MIR143/145* expression is likely not the predominant casual factor for the functional consequence of *CARMN* in maintaining SMC contractile phenotype.

SRF and its coactivator MYOCD are potent inducers of the SMC differentiation program.[10, 12] MYOCD does not bind directly to DNA, but interacts with SRF and transactivates SM-specific genes via SRF directly binding to an evolutionarily conserved CArG element.[11] We and others have shown that several factors physically interact with MYOCD to competitively displace MYOCD from SRF which prevents the binding of MYOCD/SRF complex to CArG elements, thereby inhibiting SM-specific gene expression.[71–75] While these factors are proteins and act as repressors for MYOCD function, we found for the first time, that lncRNA *Carmn* directly interacts with MYOCD, but not SRF,[62] and potentiates MYOCD function. More interestingly, *Carmn* specifically binds to the basic region and glutamine-rich region of MYOCD, the same region that is required for MYOCD interaction with SRF. We speculate that *CARMN* binding to MYOCD facilitates the binding of MYOCD and SRF, leading to enhanced transcriptional activity on SM-specific gene promoters.

In summary, we discovered that *CARMN* is a highly abundant and conserved SMC-specific lncRNA that plays a critical role in SMC differentiation through direct binding to MYOCD. Restoring or maintaining expression of *CARMN* could be a potential therapeutic approach for the treatment of proliferative vascular diseases.

Supplementary Material

Refer to Web version on PubMed Central for supplementary material.

ACKNOWLEDGMENTS

We thank Dr. Paul Herring for a critical reading of the manuscript. We also thank Drs. Qing Lyu and Joseph Miano at Vascular Biology Center of Augusta University for helpful suggestions on RNA FISH assay in mouse tissues and sharing human *SENCR* Stellaris RNA probes.

SOURCES OF FUNDING

The work at the Zhou laboratory is supported by a grant from the National Heart, Lung, and Blood Institute, NIH (R01HL149995). JZ is a recipient of Established Investigator Award (17EIA33460468) and Transformational Project Award (19TPA34910181) from the American Heart Association. AV is supported by a Merit Review Award (I01BX00389) from Department of Veterans Affairs. The content presented here does not represent the views of the Department of Veterans Affairs or the United States Government. KD and XH are supported by postdoctoral fellowships (19POST34450071 and 836341, respectively) from the American Heart Association. IO is supported by a K99 award (K99HL153896) from the National Heart, Lung, and Blood Institute, NIH.

Nonstandard Abbreviations and Acronyms:

ASO	Antisense oligonucleotide
CPC	Cardiac precursor cell

EST	Expressed sequence tag
FISH	Fluorescence *in situ* hybridization
GFP	Green fluorescent protein
GI	Gastrointestinal
GTEx	Genotype-tissue expression
GW	*CMV*-Cre^{+}/*Carmn*$^{GFP/WT}$
HCASMCs	Human coronary artery smooth muscle cells
HFD	High-fat diet
HSVSMCs	Human saphenous vein smooth muscle cells
HUVECs	Human umbilical vein endothelial cells
KI	Knock in
LncRNA	Long non-coding RNA
miR/miRNA	MicroRNA
PCW	post conception weeks
PW	Carmn$^{PFG/WT}$
RACE	Rapid amplification of cDNA ends
SA	Splicing acceptor
scRNA-seq	Single cell RNA-sequencing
RIP	RNA immunoprecipitation
ATAC-seq	Assay for Transposase Accessible Chromatin sequencing
LCA	Left carotid artery
RCA	Right carotid artery

REFERENCES

1. Miano JM and Olson EN. Expression of the smooth muscle cell calponin gene marks the early cardiac and smooth muscle cell lineages during mouse embryogenesis. J Biol Chem. 1996;271:7095–103. [PubMed: 8636144]
2. Samaha FF, Ip HS, Morrisey EE, Seltzer J, Tang Z, Solway J and Parmacek MS. Developmental pattern of expression and genomic organization of the calponin-h1 gene. A contractile smooth muscle cell marker. J Biol Chem. 1996;271:395–403. [PubMed: 8550594]
3. Wang X, Hu G, Betts C, Harmon EY, Keller RS, Van De Water L and Zhou J. Transforming growth factor-beta1-induced transcript 1 protein, a novel marker for smooth muscle contractile phenotype, is regulated by serum response factor/myocardin protein. J Biol Chem. 2011;286:41589–41599. [PubMed: 21984848]

4. Solway J, Seltzer J, Samaha FF, Kim S, Alger LE, Niu Q, Morrisey EE, Ip HS and Parmacek MS. Structure and expression of a smooth muscle cell-specific gene, SM22 alpha. J Biol Chem. 1995;270:13460–9. [PubMed: 7768949]
5. Nanda V and Miano JM. Leiomodin 1, a new serum response factor-dependent target gene expressed preferentially in differentiated smooth muscle cells. J Biol Chem. 2012;287:2459–67. [PubMed: 22157009]
6. Sawtell NM and Lessard JL. Cellular distribution of smooth muscle actins during mammalian embryogenesis: expression of the alpha-vascular but not the gamma-enteric isoform in differentiating striated myocytes. J Cell Biol. 1989;109:2929–37. [PubMed: 2687290]
7. Blue EK, Goeckeler ZM, Jin YJ, Hou L, Dixon SA, Herring BP, Wysolmerski RB and Gallagher PJ. 220-and 130-kDa MLCKs have distinct tissue distributions and intracellular localization patterns. Am J Physiol-Cell Ph. 2002;282:C451–C460.
8. Kuro-o M, Nagai R, Tsuchimochi H, Katoh H, Yazaki Y, Ohkubo A and Takaku F. Developmentally regulated expression of vascular smooth muscle myosin heavy chain isoforms. J Biol Chem. 1989;264:18272–5. [PubMed: 2681193]
9. Owens GK, Kumar MS and Wamhoff BR. Molecular regulation of vascular smooth muscle cell differentiation in development and disease. Physiol Rev. 2004;84:767–801. [PubMed: 15269336]
10. Miano JM. Serum response factor: toggling between disparate programs of gene expression. Journal of Molecular and Cellular Cardiology. 2003;35:577–593. [PubMed: 12788374]
11. Wang D, Chang PS, Wang Z, Sutherland L, Richardson JA, Small E, Krieg PA and Olson EN. Activation of cardiac gene expression by myocardin, a transcriptional cofactor for serum response factor. Cell. 2001;105:851–62. [PubMed: 11439182]
12. Wang ZG, Wang DZ, Pipes GCT and Olson EN. Myocardin is a master regulator of smooth muscle gene expression. P Natl Acad Sci USA. 2003;100:7129–7134.
13. Chen J, Kitchen CM, Streb JW and Miano JM. Myocardin: a component of a molecular switch for smooth muscle differentiation. J Mol Cell Cardiol. 2002;34:1345–56. [PubMed: 12392995]
14. Ohno S. So much'junk'DNA in our genome. Evolution of Genetic Systems, Brookhaven Symp Biol. 1972:366–370.
15. Fatica A and Bozzoni I. Long non-coding RNAs: new players in cell differentiation and development. Nature Reviews Genetics. 2014;15:7–21.
16. Han DKM, Khaing ZZ, Pollock RA, Haudenschild CC and Liau G. H19, a marker of developmental transition, is reexpressed in human atherosclerotic plaques and is regulated by the insulin family of growth factors in cultured rabbit smooth muscle cells. Journal of Clinical Investigation. 1996;97:1276–1285.
17. Bell RD, Long XC, Lin MY, Bergmann JH, Nanda V, Cowan SL, Zhou Q, Han Y, Spector DL, Zheng DY, et al. Identification and Initial Functional Characterization of a Human Vascular Cell-Enriched Long Noncoding RNA. Arterioscl Throm Vas. 2014;34:1249–1259.
18. Wu G, Cai J, Han Y, Chen J, Huang ZP, Chen C, Cai Y, Huang H, Yang Y, Liu Y, et al. LincRNA-p21 regulates neointima formation, vascular smooth muscle cell proliferation, apoptosis, and atherosclerosis by enhancing p53 activity. Circulation. 2014;130:1452–1465. [PubMed: 25156994]
19. Ballantyne MD, Pinel K, Dakin R, Vesey AT, Diver L, Mackenzie R, Garcia R, Welsh P, Sattar N, Hamilton G, et al. Smooth Muscle Enriched Long Noncoding RNA (SMILR) Regulates Cell Proliferation. Circulation. 2016;133:2050–65. [PubMed: 27052414]
20. Zhao JJ, Zhang W, Lin MY, Wu W, Jiang PT, Tou E, Xue M, Richards A, Jourd'heuil D, Asif A, et al. MYOSLID Is a Novel Serum Response Factor-Dependent Long Noncoding RNA That Amplifies the Vascular Smooth Muscle Differentiation Program. Arterioscl Throm Vas. 2016;36:2088–2099.
21. Das S, Zhang E, Senapati P, Amaram V, Reddy MA, Stapleton K, Leung A, Lanting L, Wang M, Chen Z, et al. A Novel Angiotensin II-Induced Long Noncoding RNA Giver Regulates Oxidative Stress, Inflammation, and Proliferation in Vascular Smooth Muscle Cells. Circ Res. 2018;123:1298–1312. [PubMed: 30566058]
22. Li DY, Busch A, Jin H, Chernogubova E, Pelisek J, Karlsson J, Sennblad B, Liu S, Lao S, Hofmann P, et al. H19 Induces Abdominal Aortic Aneurysm Development and Progression. Circulation. 2018;138:1551–1568. [PubMed: 29669788]

23. Lino Cardenas CL, Kessinger CW, Cheng Y, MacDonald C, MacGillivray T, Ghoshhajra B, Huleihel L, Nuri S, Yeri AS, Jaffer FA, et al. An HDAC9-MALAT1-BRG1 complex mediates smooth muscle dysfunction in thoracic aortic aneurysm. Nat Commun. 2018;9:1009. [PubMed: 29520069]
24. Lo Sardo V, Chubukov P, Ferguson W, Kumar A, Teng EL, Duran M, Zhang L, Cost G, Engler AJ, Urnov F, et al. Unveiling the Role of the Most Impactful Cardiovascular Risk Locus through Haplotype Editing. Cell. 2018;175:1796–1810 e20. [PubMed: 30528432]
25. Choi M, Lu YW, Zhao J, Wu M, Zhang W and Long X. Transcriptional control of a novel long noncoding RNA Mymsl in smooth muscle cells by a single Cis-element and its initial functional characterization in vessels. J Mol Cell Cardiol. 2020;138:147–157. [PubMed: 31751568]
26. Ahmed ASI, Dong K, Liu J, Wen T, Yu L, Xu F, Kang X, Osman I, Hu G, Bunting KM, et al. Long noncoding RNA NEAT1 (nuclear paraspeckle assembly transcript 1) is critical for phenotypic switching of vascular smooth muscle cells. Proc Natl Acad Sci U S A. 2018;115:E8660–E8667. [PubMed: 30139920]
27. Ounzain S, Micheletti R, Arnan C, Plaisance I, Cecchi D, Schroen B, Reverter F, Alexanian M, Gonzales C, Ng SY, et al. CARMEN, a human super enhancer-associated long noncoding RNA controlling cardiac specification, differentiation and homeostasis. J Mol Cell Cardiol. 2015;89:98–112. [PubMed: 26423156]
28. Plaisance I, Perruchoud S, Fernandez-Tenorio M, Gonzales C, Ounzain S, Ruchat P, Nemir M, Niggli E and Pedrazzini T. Cardiomyocyte Lineage Specification in Adult Human Cardiac Precursor Cells Via Modulation of Enhancer-Associated Long Noncoding RNA Expression. JACC Basic Transl Sci. 2016;1:472–493. [PubMed: 29707678]
29. Cheng YH, Liu XJ, Yang J, Lin Y, Xu DZ, Lu Q, Deitch EA, Huo YQ, Delphin ES and Zhang CX. MicroRNA-145, a Novel Smooth Muscle Cell Phenotypic Marker and Modulator, Controls Vascular Neointimal Lesion Formation. Circulation Research. 2009;105:158–U113. [PubMed: 19542014]
30. Cordes KR, Sheehy NT, White MP, Berry EC, Morton SU, Muth AN, Lee TH, Miano JM, Ivey KN and Srivastava D. miR-145 and miR-143 regulate smooth muscle cell fate and plasticity. Nature. 2009;460:705–10. [PubMed: 19578358]
31. Elia L, Quintavalle M, Zhang J, Contu R, Cossu L, Latronico MV, Peterson KL, Indolfi C, Catalucci D, Chen J, et al. The knockout of miR-143 and −145 alters smooth muscle cell maintenance and vascular homeostasis in mice: correlates with human disease. Cell Death Differ. 2009;16:1590–8. [PubMed: 19816508]
32. Xin M, Small EM, Sutherland LB, Qi X, McAnally J, Plato CF, Richardson JA, Bassel-Duby R and Olson EN. MicroRNAs miR-143 and miR-145 modulate cytoskeletal dynamics and responsiveness of smooth muscle cells to injury. Genes Dev. 2009;23:2166–78. [PubMed: 19720868]
33. Wang X, Hu G and Zhou J. Repression of versican expression by microRNA-143. J Biol Chem. 2010;285:23241–50. [PubMed: 20489207]
34. Boettger T, Beetz N, Kostin S, Schneider J, Kruger M, Hein L and Braun T. Acquisition of the contractile phenotype by murine arterial smooth muscle cells depends on the Mir143/145 gene cluster. J Clin Invest. 2009;119:2634–47. [PubMed: 19690389]
35. Wirka RC, Wagh D, Paik DT, Pjanic M, Nguyen T, Miller CL, Kundu R, Nagao M, Coller J, Koyano TK, et al. Atheroprotective roles of smooth muscle cell phenotypic modulation and the TCF21 disease gene as revealed by single-cell analysis. Nat Med. 2019;25:1280–1289. [PubMed: 31359001]
36. Armulik A, Genove G and Betsholtz C. Pericytes: developmental, physiological, and pathological perspectives, problems, and promises. Dev Cell. 2011;21:193–215. [PubMed: 21839917]
37. Hall IF, Climent M, Quintavalle M, Farina FM, Schorn T, Zani S, Carullo P, Kunderfranco P, Civilini E, Condorelli G, et al. Circ_Lrp6, a Circular RNA Enriched in Vascular Smooth Muscle Cells, Acts as a Sponge Regulating miRNA-145 Function. Circulation Research. 2019;124:498–510. [PubMed: 30582454]
38. You X, Vlatkovic I, Babic A, Will T, Epstein I, Tushev G, Akbalik G, Wang M, Glock C, Quedenau C, et al. Neural circular RNAs are derived from synaptic genes and regulated by development and plasticity. Nat Neurosci. 2015;18:603–610. [PubMed: 25714049]

39. Kalluri AS, Vellarikkal SK, Edelman ER, Nguyen L, Subramanian A, Ellinor PT, Regev A, Kathiresan S and Gupta RM. Single-Cell Analysis of the Normal Mouse Aorta Reveals Functionally Distinct Endothelial Cell Populations. Circulation. 2019;140:147–163. [PubMed: 31146585]
40. Dobnikar L, Taylor AL, Chappell J, Oldach P, Harman JL, Oerton E, Dzierzak E, Bennett MR, Spivakov M and Jorgensen HF. Disease-relevant transcriptional signatures identified in individual smooth muscle cells from healthy mouse vessels. Nat Commun. 2018;9:4567. [PubMed: 30385745]
41. Lee G and Saito I. Role of nucleotide sequences of loxP spacer region in Cre-mediated recombination. Gene. 1998;216:55–65. [PubMed: 9714735]
42. Li G, Tian L, Goodyer W, Kort EJ, Buikema JW, Xu A, Wu JC, Jovinge S and Wu SM. Single cell expression analysis reveals anatomical and cell cycle-dependent transcriptional shifts during heart development. Development. 2019;146.
43. Kannan S, Miyamoto M, Lin BL, Zhu R, Murphy S, Kass DA, Andersen P and Kwon C. Large Particle Fluorescence-Activated Cell Sorting Enables High-Quality Single-Cell RNA Sequencing and Functional Analysis of Adult Cardiomyocytes. Circ Res. 2019;125:567–569. [PubMed: 31415233]
44. Skelly DA, Squiers GT, McLellan MA, Bolisetty MT, Robson P, Rosenthal NA and Pinto AR. Single-Cell Transcriptional Profiling Reveals Cellular Diversity and Intercommunication in the Mouse Heart. Cell Rep. 2018;22:600–610. [PubMed: 29346760]
45. Asp M, Giacomello S, Larsson L, Wu C, Furth D, Qian X, Wardell E, Custodio J, Reimegard J, Salmen F, et al. A Spatiotemporal Organ-Wide Gene Expression and Cell Atlas of the Developing Human Heart. Cell. 2019;179:1647–1660 e19. [PubMed: 31835037]
46. Wang L, Yu P, Zhou B, Song J, Li Z, Zhang M, Guo G, Wang Y, Chen X, Han L, et al. Single-cell reconstruction of the adult human heart during heart failure and recovery reveals the cellular landscape underlying cardiac function. Nat Cell Biol. 2020;22:108–119. [PubMed: 31915373]
47. Ayari H and Bricca G. Identification of two genes potentially associated in iron-heme homeostasis in human carotid plaque using microarray analysis. J Biosci. 2013;38:311–5. [PubMed: 23660665]
48. Bekelis K, Kerley-Hamilton JS, Teegarden A, Tomlinson CR, Kuintzle R, Simmons N, Singer RJ, Roberts DW, Kellis M and Hendrix DA. MicroRNA and gene expression changes in unruptured human cerebral aneurysms. J Neurosurg. 2016;125:1390–1399. [PubMed: 26918470]
49. Miller CL, Pjanic M, Wang T, Nguyen T, Cohain A, Lee JD, Perisic L, Hedin U, Kundu RK, Majmudar D, et al. Integrative functional genomics identifies regulatory mechanisms at coronary artery disease loci. Nature Communications. 2016;7:12092.
50. Hu Y, Zhang Z, Torsney E, Afzal AR, Davison F, Metzler B and Xu Q. Abundant progenitor cells in the adventitia contribute to atherosclerosis of vein grafts in ApoE-deficient mice. J Clin Invest. 2004;113:1258–65. [PubMed: 15124016]
51. Frid MG, Kale VA and Stenmark KR. Mature vascular endothelium can give rise to smooth muscle cells via endothelial-mesenchymal transdifferentiation - In vitro analysis. Circulation Research. 2002;90:1189–1196. [PubMed: 12065322]
52. Liu MJ and Gomez D. Smooth Muscle Cell Phenotypic Diversity At the Crossroads of Lineage Tracing and Single-Cell Transcriptomics. Arterioscl Throm Vas. 2019;39:1715–1723.
53. Pan H, Xue C, Auerbach BJ, Fan J, Bashore AC, Cui J, Yang DY, Trignano SB, Liu W, Shi J, et al. Single-Cell Genomics Reveals a Novel Cell State During Smooth Muscle Cell Phenotypic Switching and Potential Therapeutic Targets for Atherosclerosis in Mouse and Human. Circulation. 2020;142:2060–2075. [PubMed: 32962412]
54. Holycross BJ, Blank RS, Thompson MM, Peach MJ and Owens GK. Platelet-derived growth factor-BB-induced suppression of smooth muscle cell differentiation. Circ Res. 1992;71:1525–32. [PubMed: 1423945]
55. Herring BP, Hoggatt AM, Burlak C and Offermanns S. Previously differentiated medial vascular smooth muscle cells contribute to neointima formation following vascular injury. Vasc Cell. 2014;6:21. [PubMed: 25309723]
56. Gil N and Ulitsky I. Regulation of gene expression by cis-acting long non-coding RNAs. Nat Rev Genet. 2020;21:102–117. [PubMed: 31729473]

57. Anderson KM, Anderson DM, McAnally JR, Shelton JM, Bassel-Duby R and Olson EN. Transcription of the non-coding RNA upperhand controls Hand2 expression and heart development. Nature. 2016;539:433–436. [PubMed: 27783597]
58. Muppirala UK, Honavar VG and Dobbs D. Predicting RNA-Protein Interactions Using Only Sequence Information. Bmc Bioinformatics. 2011;12:489. [PubMed: 22192482]
59. Lyu Q, Dhagia V, Han Y, Guo B, Wines-Samuelson ME, Christie CK, Yin Q, Slivano OJ, Herring P, Long X, et al. CRISPR-Cas9-Mediated Epitope Tagging Provides Accurate and Versatile Assessment of Myocardin-Brief Report. Arterioscler Thromb Vasc Biol. 2018;38:2184–2190. [PubMed: 29976770]
60. Zhou J, Zhang M, Fang H, El-Mounayri O, Rodenberg JM, Imbalzano AN and Herring BP. The SWI/SNF chromatin remodeling complex regulates myocardin-induced smooth muscle-specific gene expression. Arterioscler Thromb Vasc Biol. 2009;29:921–8. [PubMed: 19342595]
61. Vacante F, Rodor J, Lalwani MK, Mahmoud AD, Bennett M, De Pace AL, Miller E, Van Kuijk K, de Bruijn J, Gijbels M, et al. CARMN Loss Regulates Smooth Muscle Cells and Accelerates Atherosclerosis in Mice. Circ Res. 2021;128:1258–1275. [PubMed: 33622045]
62. Ni H, Haemmig S, Deng Y, Chen J, Simion V, Yang D, Sukhova G, Shvartz E, Wara A, Cheng HS, et al. A Smooth Muscle Cell-Enriched Long Noncoding RNA Regulates Cell Plasticity and Atherosclerosis by Interacting With Serum Response Factor. Arterioscler Thromb Vasc Biol. 2021;41:2399–2416. [PubMed: 34289702]
63. Kramann R, Goettsch C, Wongboonsin J, Iwata H, Schneider RK, Kuppe C, Kaesler N, Chang-Panesso M, Machado FG, Gratwohl S, et al. Adventitial MSC-like Cells Are Progenitors of Vascular Smooth Muscle Cells and Drive Vascular Calcification in Chronic Kidney Disease. Cell Stem Cell. 2016;19:628–642. [PubMed: 27618218]
64. Wang H, Zhao H, Zhu H, Li Y, Tang J, Li Y and Zhou B. Sca1(+) Cells Minimally Contribute to Smooth Muscle Cells in Atherosclerosis. Circ Res. 2021;128:133–135. [PubMed: 33146591]
65. Tang J, Wang H, Huang X, Li F, Zhu H, Li Y, He L, Zhang H, Pu W, Liu K, et al. Arterial Sca1(+) Vascular Stem Cells Generate De Novo Smooth Muscle for Artery Repair and Regeneration. Cell Stem Cell. 2020;26:81–96 e4. [PubMed: 31883835]
66. Wan M, Li C, Zhen G, Jiao K, He W, Jia X, Wang W, Shi C, Xing Q, Chen YF, et al. Injury-activated transforming growth factor beta controls mobilization of mesenchymal stem cells for tissue remodeling. Stem Cells. 2012;30:2498–511. [PubMed: 22911900]
67. Yuan F, Wang D, Xu K, Wang J, Zhang Z, Yang L, Yang GY and Li S. Contribution of Vascular Cells to Neointimal Formation. PLoS One. 2017;12:e0168914.
68. Rangrez AY, Massy ZA, Metzinger-Le Meuth V and Metzinger L. miR-143 and miR-145: molecular keys to switch the phenotype of vascular smooth muscle cells. Circ Cardiovasc Genet. 2011;4:197–205. [PubMed: 21505201]
69. Zhou VW, Goren A and Bernstein BE. Charting histone modifications and the functional organization of mammalian genomes. Nat Rev Genet. 2011;12:7–18. [PubMed: 21116306]
70. Carmona S, Lin B, Chou T, Arroyo K and Sun S. LncRNA Jpx induces Xist expression in mice using both trans and cis mechanisms. Plos Genetics. 2018;14.
71. Zhou J, Hu G and Wang X. Repression of smooth muscle differentiation by a novel high mobility group box-containing protein, HMG2L1. J Biol Chem. 2010;285:23177–85. [PubMed: 20511232]
72. Zhou J, Blue EK, Hu G and Herring BP. Thymine DNA glycosylase represses myocardin-induced smooth muscle cell differentiation by competing with serum response factor for myocardin binding. J Biol Chem. 2008;283:35383–92. [PubMed: 18945672]
73. Zheng JP, He X, Liu F, Yin S, Wu S, Yang M, Zhao J, Dai X, Jiang H, Yu L, et al. YY1 directly interacts with myocardin to repress the triad myocardin/SRF/CArG box-mediated smooth muscle gene transcription during smooth muscle phenotypic modulation. Sci Rep. 2020;10:21781. [PubMed: 33311559]
74. Liu Y, Sinha S, McDonald OG, Shang Y, Hoofnagle MH and Owens GK. Kruppel-like factor 4 abrogates myocardin-induced activation of smooth muscle gene expression. J Biol Chem. 2005;280:9719–27. [PubMed: 15623517]

75. Tang RH, Zheng XL, Callis TE, Stansfield WE, He J, Baldwin AS, Wang DZ and Selzman CH. Myocardin inhibits cellular proliferation by inhibiting NF-kappaB(p65)-dependent cell cycle progression. Proc Natl Acad Sci U S A. 2008;105:3362–7. [PubMed: 18296632]
76. Maass PG, Glazar P, Memczak S, Dittmar G, Hollfinger I, Schreyer L, Sauer AV, Toka O, Aiuti A, Luft FC, et al. A map of human circular RNAs in clinically relevant tissues. J Mol Med (Berl). 2017;95:1179–1189. [PubMed: 28842720]
77. Bolger AM, Lohse M and Usadel B. Trimmomatic: a flexible trimmer for Illumina sequence data. Bioinformatics. 2014;30:2114–20. [PubMed: 24695404]
78. Kim D, Pertea G, Trapnell C, Pimentel H, Kelley R and Salzberg SL. TopHat2: accurate alignment of transcriptomes in the presence of insertions, deletions and gene fusions. Genome Biol. 2013;14:R36. [PubMed: 23618408]
79. Trapnell C, Roberts A, Goff L, Pertea G, Kim D, Kelley DR, Pimentel H, Salzberg SL, Rinn JL and Pachter L. Differential gene and transcript expression analysis of RNA-seq experiments with TopHat and Cufflinks. Nat Protoc. 2012;7:562–78. [PubMed: 22383036]
80. Liao Y, Smyth GK and Shi W. featureCounts: an efficient general purpose program for assigning sequence reads to genomic features. Bioinformatics. 2014;30:923–30. [PubMed: 24227677]
81. Mortazavi A, Williams BA, McCue K, Schaeffer L and Wold B. Mapping and quantifying mammalian transcriptomes by RNA-Seq. Nat Methods. 2008;5:621–8. [PubMed: 18516045]
82. Hong EL, Sloan CA, Chan ET, Davidson JM, Malladi VS, Strattan JS, Hitz BC, Gabdank I, Narayanan AK, Ho M, et al. Principles of metadata organization at the ENCODE data coordination center. Database-Oxford. 2016; 1–10.
83. Butler A, Hoffman P, Smibert P, Papalexi E and Satija R. Integrating single-cell transcriptomic data across different conditions, technologies, and species. Nat Biotechnol. 2018;36:411–420. [PubMed: 29608179]
84. Thorvaldsdottir H, Robinson JT and Mesirov JP. Integrative Genomics Viewer (IGV): high-performance genomics data visualization and exploration. Brief Bioinform. 2013;14:178–92. [PubMed: 22517427]
85. Langmead B and Salzberg SL. Fast gapped-read alignment with Bowtie 2. Nat Methods. 2012;9:357–9. [PubMed: 22388286]
86. Zhang Y, Liu T, Meyer CA, Eeckhoute J, Johnson DS, Bernstein BE, Nusbaum C, Myers RM, Brown M, Li W, et al. Model-based analysis of ChIP-Seq (MACS). Genome Biol. 2008;9:R137. [PubMed: 18798982]
87. Love MI, Huber W and Anders S. Moderated estimation of fold change and dispersion for RNA-seq data with DESeq2. Genome Biol. 2014;15:550. [PubMed: 25516281]
88. Lyu Q, Xu SW, Lyu YY, Choi M, Christie CK, Slivano OJ, Rahman A, Jin ZG, Long XC, Xu YW, et al. SENCR stabilizes vascular endothelial cell adherens junctions through interaction with CKAP4. P Natl Acad Sci USA. 2019;116:546–555.
89. Wen T, Liu J, He X, Dong K, Hu G, Yu L, Yin Q, Osman I, Peng J, Zheng Z, et al. Transcription factor TEAD1 is essential for vascular development by promoting vascular smooth muscle differentiation. Cell Death Differ. 2019;26:2790–2806. [PubMed: 31024075]
90. Liu F, Wang X, Hu G, Wang Y and Zhou J. The transcription factor TEAD1 represses smooth muscle-specific gene expression by abolishing myocardin function. J Biol Chem. 2014;289:3308–16. [PubMed: 24344135]
91. Xu F, Ahmed AI, Kang XH, Hu GQ, Liu F, Zhang W and Zhou JL. MicroRNA-15b/16 Attenuates Vascular Neointima Formation by Promoting the Contractile Phenotype of Vascular Smooth Muscle Through Targeting YAP. Arterioscl Throm Vas. 2015;35:2145–2152.
92. Osman I, He X, Liu J, Dong K, Wen T, Zhang F, Yu L, Hu G, Xin H, Zhang W, et al. TEAD1 (TEA Domain Transcription Factor 1) Promotes Smooth Muscle Cell Proliferation Through Upregulating SLC1A5 (Solute Carrier Family 1 Member 5)-Mediated Glutamine Uptake. Circ Res. 2019;124:1309–1322. [PubMed: 30801233]
93. Wang X, Hu G, Gao X, Wang Y, Zhang W, Harmon EY, Zhi X, Xu Z, Lennartz MR, Barroso M, et al. The induction of yes-associated protein expression after arterial injury is crucial for smooth muscle phenotypic modulation and neointima formation. Arterioscler Thromb Vasc Biol. 2012;32:2662–9. [PubMed: 22922963]

94. Wirth A, Benyo Z, Lukasova M, Leutgeb B, Wettschureck N, Gorbey S, Orsy P, Horvath B, Maser-Gluth C, Greiner E, et al. G12-G13-LARG-mediated signaling in vascular smooth muscle is required for salt-induced hypertension. Nat Med. 2008;14:64–8. [PubMed: 18084302]

95. Clowes AW, Reidy MA and Clowes MM. Kinetics of cellular proliferation after arterial injury. I. Smooth muscle growth in the absence of endothelium. Lab Invest. 1983;49:327–33. [PubMed: 6887785]

96. Herring BP, Kriegel AM and Hoggatt AM. Identification of Barx2b, a serum response factor-associated homeodomain protein. J Biol Chem. 2001;276:14482–9. [PubMed: 11278942]

97. Zhou J and Herring BP. Mechanisms responsible for the promoter-specific effects of myocardin. J Biol Chem. 2005;280:10861–9. [PubMed: 15657056]

CLINICAL PERSPECTIVE

What is new?

- *CARMN* is a SMC-specific lncRNA that promotes the contractile phenotype of SMCs, independent of *MIR143/145*.
- SMC-specific deletion of *Carmn* exacerbates while over-expression of *CARMN* attenuates injury-induced neointima formation and SMC dedifferentiation.
- *CARMN* is the first non-coding RNA discovered to interact with the SMC-specific transcriptional cofactor, myocardin.

What are the clinical implications?

- Our study provides novel insights into the mechanisms underlying SMC phenotypic modulation that contributes to the development of vascular diseases such as atherosclerosis and restenosis after angioplasty.
- Restoration of *CARMN* expression in susceptible individuals may be a promising therapeutic approach for the treatment of SMC-driven vascular diseases.

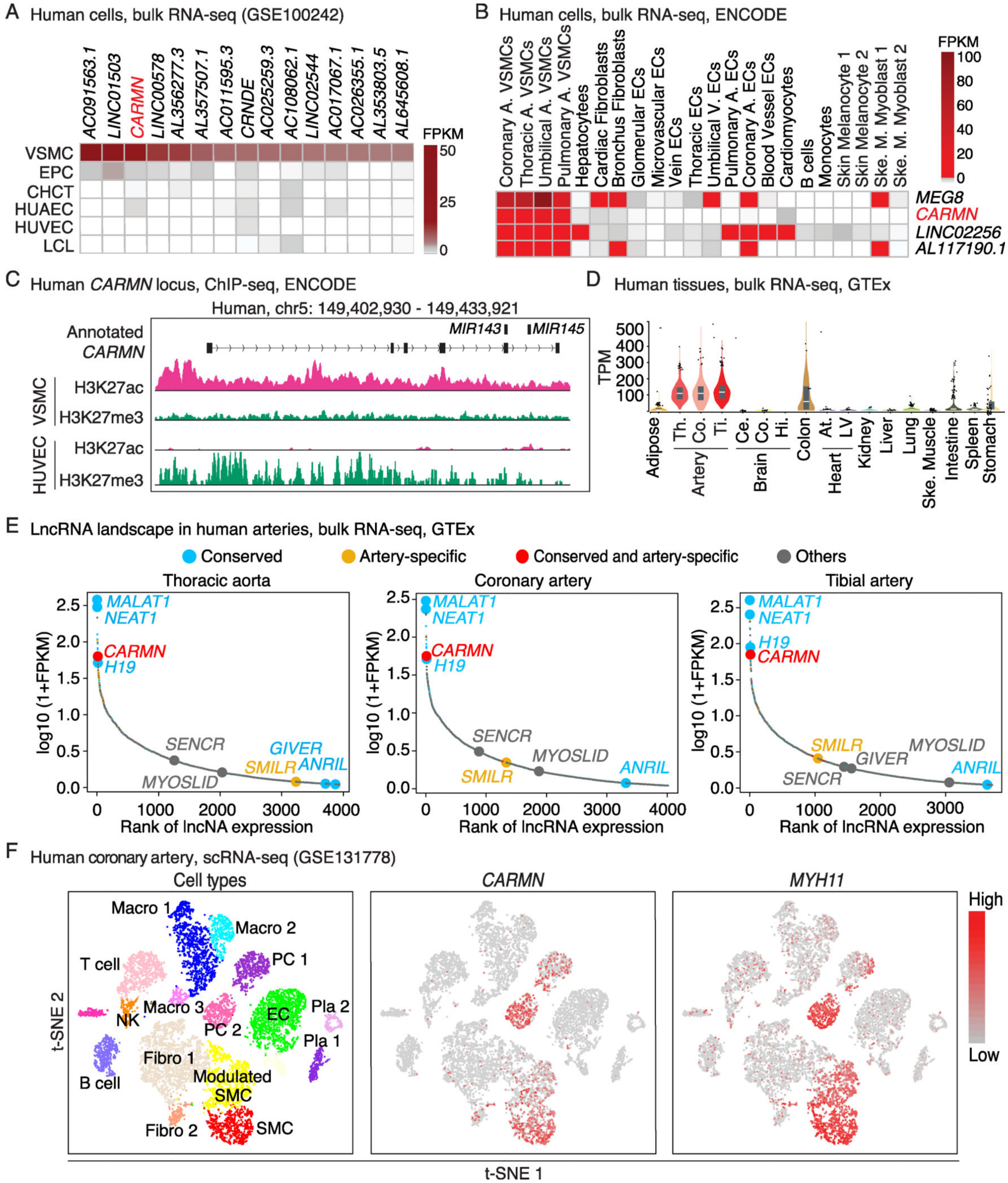

Figure 1. Transcriptome analysis reveals *CARMN* is a highly abundant SMC-specific lncRNA in human.

(**A**) Heatmap showing 15 VSMC-enriched lncRNAs identified by the publicly available human RNA-seq dataset (GSE100242). EPC: endothelial progenitor cells; CHCT: chondrocytes; HUAEC: human aortic endothelial cells; HUVEC: human umbilical vein endothelial cells; LCL: lymphoblastoid cell line. FPKM: Fragments Per Kilobase of transcript per Million mapped reads. (**B**) Heatmap showing 4 VSMC-enriched lncRNAs in 22 primary human cell types retrieved from the ENCODE database. A: artery; V: Vein; ECs:

endothelial cells; Ske. M.: Skeletal Muscle. (**C**) ChIP-seq tracks of histone 3 modifications at the human *CARMN* locus in aortic VSMC vs HUVEC as revealed by the ENCODE project. Y-axis scale: 20 for H3K27ac and 5 for H3K27me3. (**D**) *CARMN* expression in human tissues was revealed by the GTEx database. Th: thoracic aorta; Co: coronary artery; Ti: tibial artery; Ce: cerebellum; Co: cortex; Hi.: hippocampus; At: atrium; LV: left ventricle. TPM: Transcripts Per kilobase Million. (**E**) The lncRNA landscape in human thoracic aorta (left), coronary artery (middle) and tibial artery (right) revealed by bulk RNA-seq from GTEx database. Annotated dots indicate lncRNAs which have been investigated in VSMCs. (**F**) t-SNE (t-distributed Stochastic Neighbor Embedding) visualization of cell types isolated from the right coronary artery of four human patients (left), and the expression of *CARMN* (middle) and *MYH11* (right) revealed by the scRNA-seq analysis (GSE131778). The color scale on the right indicates the expression levels of both *CARMN* and *MYH11.* Fibro: fibroblast; EC: endothelial cell; PC: pericyte cell; Macro: macrophage; NK: natural killer cell; Pla: plasma cell.

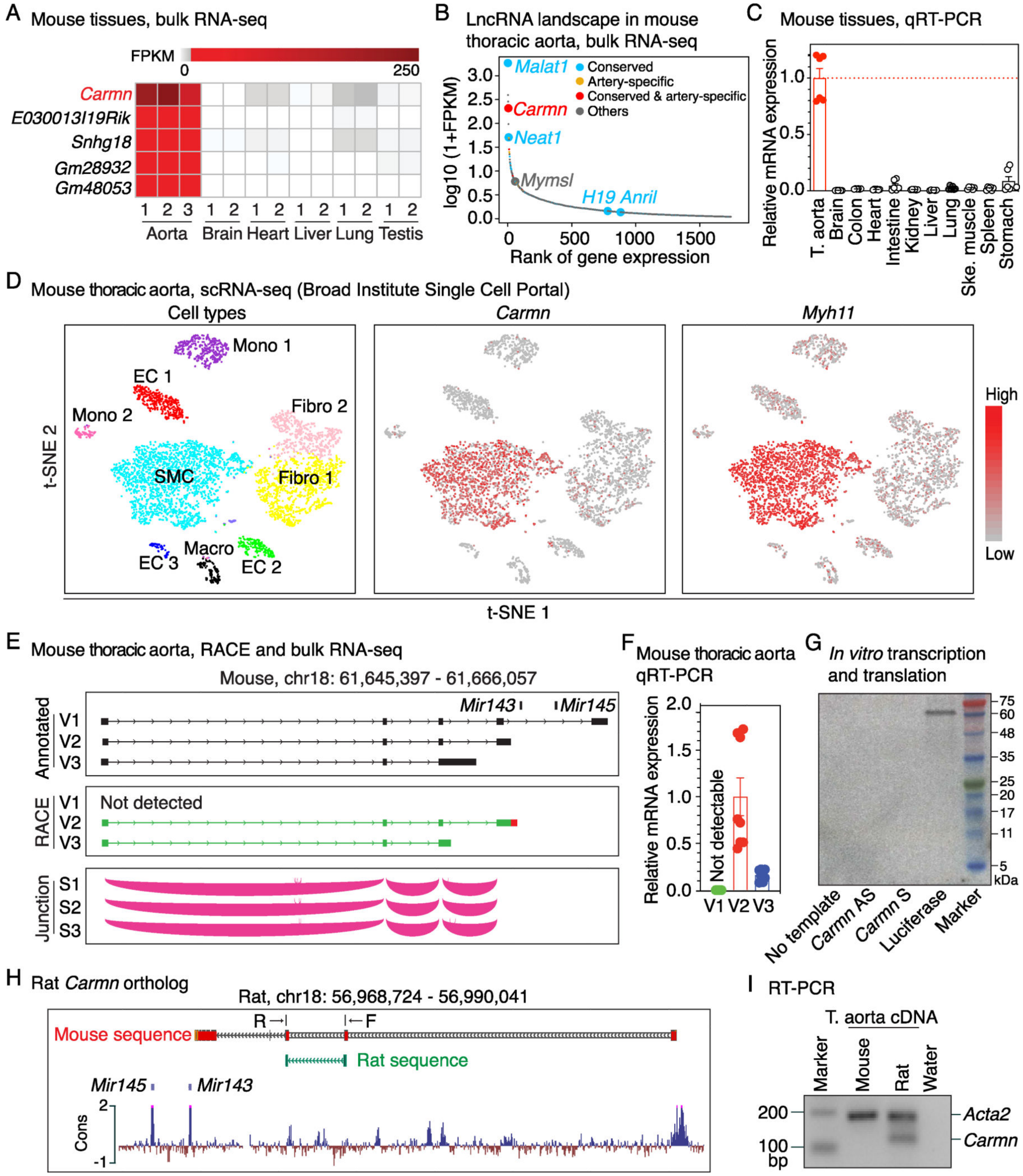

Figure 2. *CARMN* is a SMC-specific lncRNA in mouse.

(**A**) Heatmap showing the aorta-enriched lncRNAs identified by RNA-seq data of different mouse tissues. (**B**) The lncRNA landscape in mouse thoracic aorta revealed by RNA-seq. Annotated dots indicate lncRNAs which have been implicated in VSMCs. (**C**) *Carmn* expression was assessed in different mouse tissues by qRT-PCR. The expression of *Carmn* in mouse thoracic (T.) aorta was set to 1 (dashed line). Ske.: skeletal. N=6. (**D**) t-SNE visualization of cell types present in normal mouse thoracic aorta (left) and the expression of *Carmn* (middle) and *Myh11* (right) revealed by scRNA-seq (Broad Institute Single Cell

Portal). Mono: monocyte. (**E**) *Carmn* transcripts (V1–3) were identified by RACE (middle panel) in comparison with the annotated *Carmn* variants in UCSC genome browser (upper panel). The Sashimi plot is to visualize the splice junctions of *Carmn* in mouse aorta (bottom panel; N=3; S1–3). (**F**) qRT-PCR validated that V2 is the most abundant transcript in mouse thoracic aorta. N=6. **(G)** *In vitro* transcription and translation of sense or antisense mouse *Carmn* transcript V2. Plasmid encoding luciferase is used as a positive control and the reaction with no DNA template is used as an additional negative control. **(H)** Determination of rat *Carmn* ortholog. The mouse *Carmn* transcript V2 sequence was used as a query sequence to perform BLAST against rat genome. A putative rat *Carmn* ortholog positionally conserved to *miR143/145* locus, was obtained (mouse sequence in red). A pair of primers (F: forward; R: reverse) specifically targeting two different putative exons of rat *Carmn* gene were designed and used for PCR amplification with rat aorta cDNA as template. The obtained PCR product was subjected to Sanger sequencing for mapping back to rat genome by BLAST (rat sequence, green). The conservation tracks of 20 vertebrates in the putative rat *Carmn* gene locus are shown at the bottom panel. (**I**) Gel picture of PCR product showing that PCR with rat specific primers indicated in "**H**" (F and R) specifically generated a product from rat thoracic (T.) aorta cDNA, but not from mouse or water. Primers for both rat and mouse *Acta2* were used as an internal control for PCR. Water was used as a negative control.

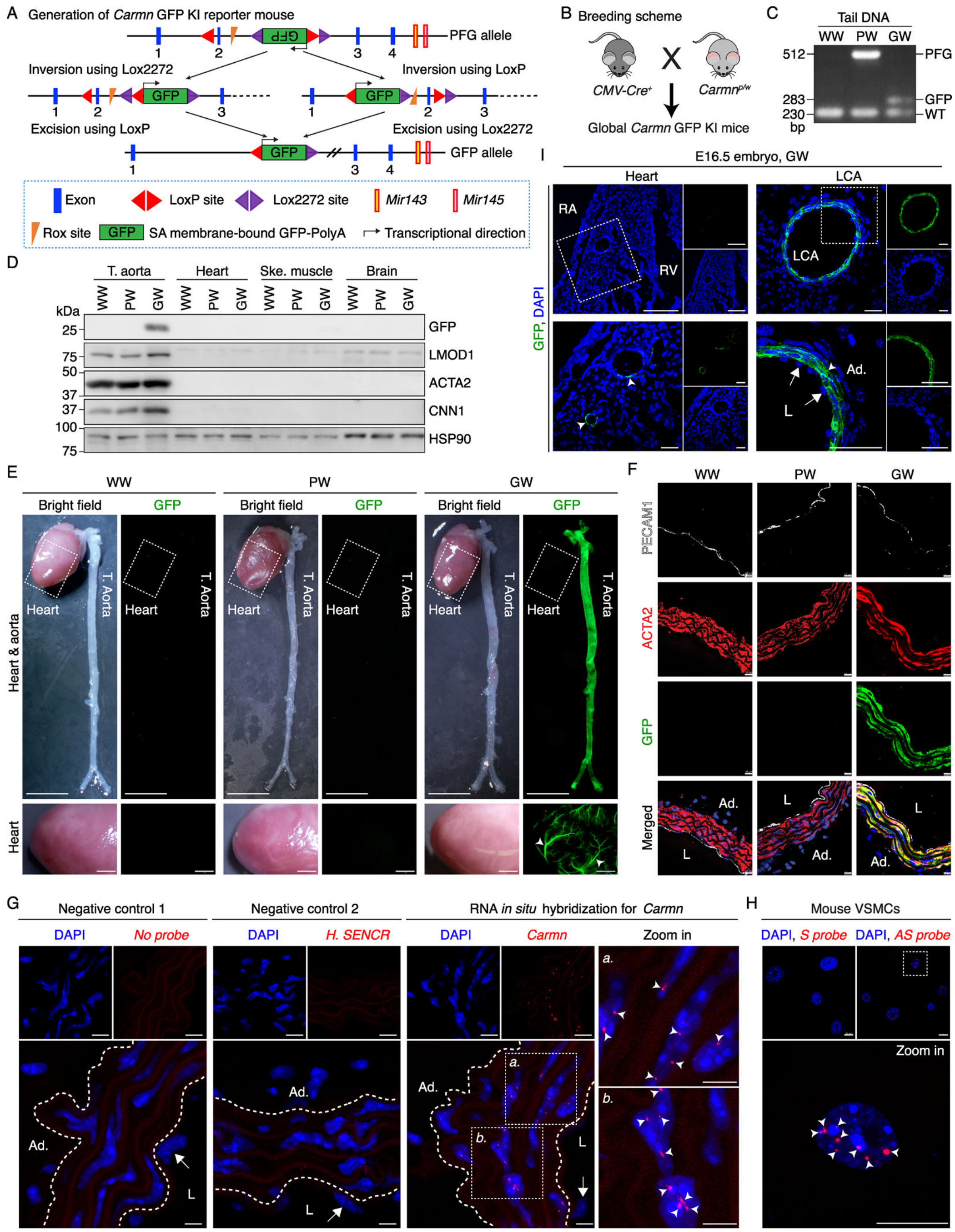

Figure 3. Visualization of SMC-specific expression of *Carmn in vivo*.

(**A**) Strategy used to generate the *Carmn* GFP KI mouse model showing the inverted GFP KI cassette in the *Carmn* gene locus. SA: splicing acceptor site. (**B**) The breeding strategy to generate global *Carmn* GFP KI mice. (**C**) PCR analysis of genomic DNA showing recombination of the *Carmn* gene in tail DNA extracted from WW, PW and GW mice. (**D**) Western blot showing GFP expression specifically in thoracic aorta (T) of GW mice. Ske: skeletal. (**E**) Heart and aorta were dissected from adult WW, PW and GW mice and photographed under bright field or GFP channel. T. aorta: thoracic aorta.

Scale bar: 5 mm and 1 mm in upper and bottom panel, respectively. The arrowheads point to the representative coronary arteries in the GW mouse heart. (**F**) Immuno-staining was performed to examine the specific cellular localization of GFP in thoracic aorta dissected from WW, PW and GW mice. L: lumen. Ad: adventitial layer. Scale bar: 10 μm. (**G**) RNA-FISH was carried out to visualize *Carmn* (red) in adult mouse thoracic aorta. The sections hybridized with hybridization buffer only (left), human-specific antisense (AS) *SENCR* probe (middle) were used as negative controls. Cell nuclei were counter stained with DAPI (blue). Dashed lines indicate external or internal elastic lamina. The boxed areas (*a* and *b*) are magnified to the right. Arrows point to endothelial cells and arrowheads indicate *Carmn* signal, respectively. L: lumen; Ad: adventitial layer. Scale bar: 10 μm. (**H**) *Carmn* subcellular localization in mouse VSMCs transduced with *Carmn* adenovirus was revealed by RNA-FISH using *Carmn* AS probe (red). *Carmn* sense probe (S) was used as negative control. Cell nuclei were stained with DAPI (blue). The boxed area is magnified below. Arrowheads indicate *Carmn* signal. Scale bar: 20 μm. (**I**) Visualization of GFP expression in E16.5 GW embryos showing that GFP is specifically expressed in arteriolar SMCs in right ventricle (RV) and medial SMCs (arrowheads) of left common carotid artery (LCA) but not in cardiomyocytes, endothelium (arrows) or adventitial (Ad.) cells. The boxed area is magnified below. RA: right atrium; L: lumen; Ad: adventitial layer. Scale bar: 20 μm.

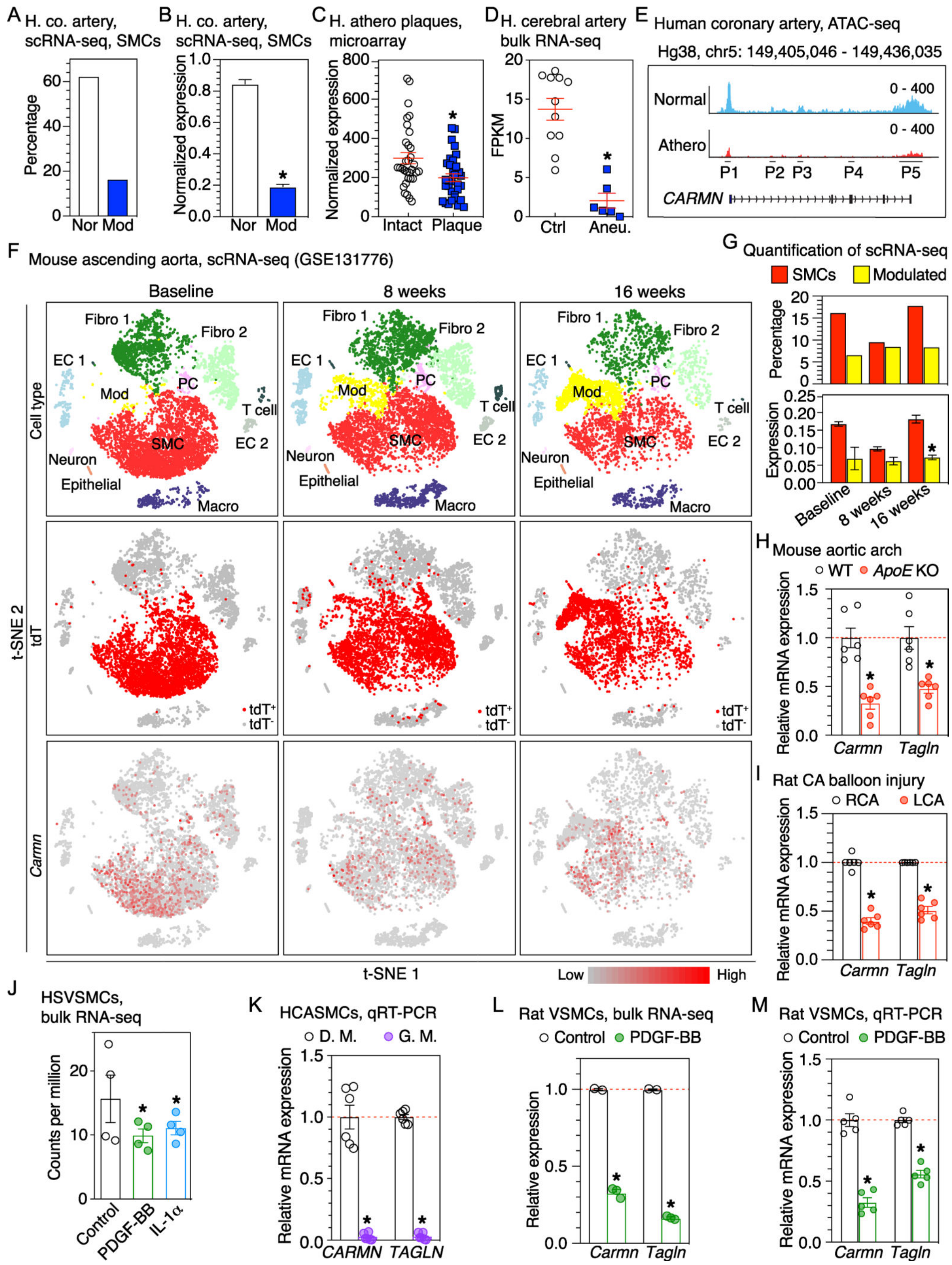

Figure 4. *CARMN* expression is down-regulated in human VSMC-related diseases, rodent vascular disease models and in VSMCs in response to stimuli of phenotypic modulation.

(**A**) Quantitative analysis of the percentage of *CARMN* positive cells (non-zero) and (**B**) expression level of *CARMN* in normal (Nor) and modulated (Mod) SMC clusters revealed by scRNA-seq of diseased human (H.) coronary (co.) artery as shown in Figure 1F. *FDR < 0.05; differential analysis with Seurat package. (**C**) Re-analysis of previously reported microarray or bulk RNA-seq datasets showing *CARMN* expression significantly decreased in diseased human arteries such as atherosclerotic arteries (GSE43292, N=32) and (**D**) cerebral arteries with aneurysm (Aneu.) (GSE66240, N=6–11), respectively. Ctrl: control. *FDR < 0.05; differential analysis with the GEO2R online tool for microarray data and DESeq2 package for bulk RNA-seq data. **(E)** Re-analysis of ATAC-seq dataset (GSE72696) showing intensity of ATAC-seq peaks (P1–5) at *CARMN* gene locus exhibits a notable decrease in human atherosclerotic coronary artery as compared to normal coronary arteries (representative picture of 1 out of 3 samples). N=3; differential analysis with DESeq2 package. (**F**) t-SNE visualization of cell types (upper), SMC lineage-traced cells (middle), and *Carmn* expression (bottom) of scRNA-seq data from aortic root and ascending aorta of *Rosa26*$^{\text{tdTomato+}}$; *ApoE*$^{-/-}$; *Myh11*-CreER^{T2} mice at baseline, 8 and 16 weeks after HFD feeding (GSE131776). Mod: modulated SMCs. **(G)** Quantitative analysis of percentage of *Carmn* positive cells (non-zero, upper) and expression level of *Carmn* (bottom) in normal and modulated SMC clusters (including both tdTomato positive and negative cells). *FDR < 0.05; differential analysis with Seurat package. (**H**) qRT-PCR analysis of expression of *Carmn* and SM-specific gene *Tagln* in lesion-laden aortic arch in *ApoE*$^{-/-}$ mice following western-diet for 12 weeks or in chow diet-fed control WT mice. N=6; *P < 0.05; unpaired Student's t-test. (**I**) qRT-PCR analysis of *Carmn* and *Tagln* expression in balloon-injured rat left carotid artery (LCA). Uninjured right CA (RCA) served as control (set to 1). N=6; *P < 0.05; unpaired Student's t-test. (**J**) Re-analysis of public RNA-seq data showing decreased expression of *CARMN* upon stimulation of PDGF-BB or IL-1α in human saphenous vein (HSV) SMCs. N=4; *FDR < 0.05; differential analysis with DESeq2 package. (**K**) qRT-PCR to show *CARMN* and *TAGLN* expression in HCASMCs cultured with differentiation medium (D.M., set to 1) or growth medium (G.M.) for 48 hours. N=6; *P < 0.05; unpaired Student's t-test. **(L)** Re-analysis of public RNA-seq data showing reduced expression of *Carmn* in rat VSMCs treated with PDGF-BB for 24 hours. N=2–3; *FDR < 0.05; differential analysis with DESeq2 package. (**M**) qRT-PCR analysis of *Carmn* expression in rat VSMCs treated with PDGF-BB (50 ng/ml) for 24 hours. N=5; *P < 0.05; unpaired Student's t-test.

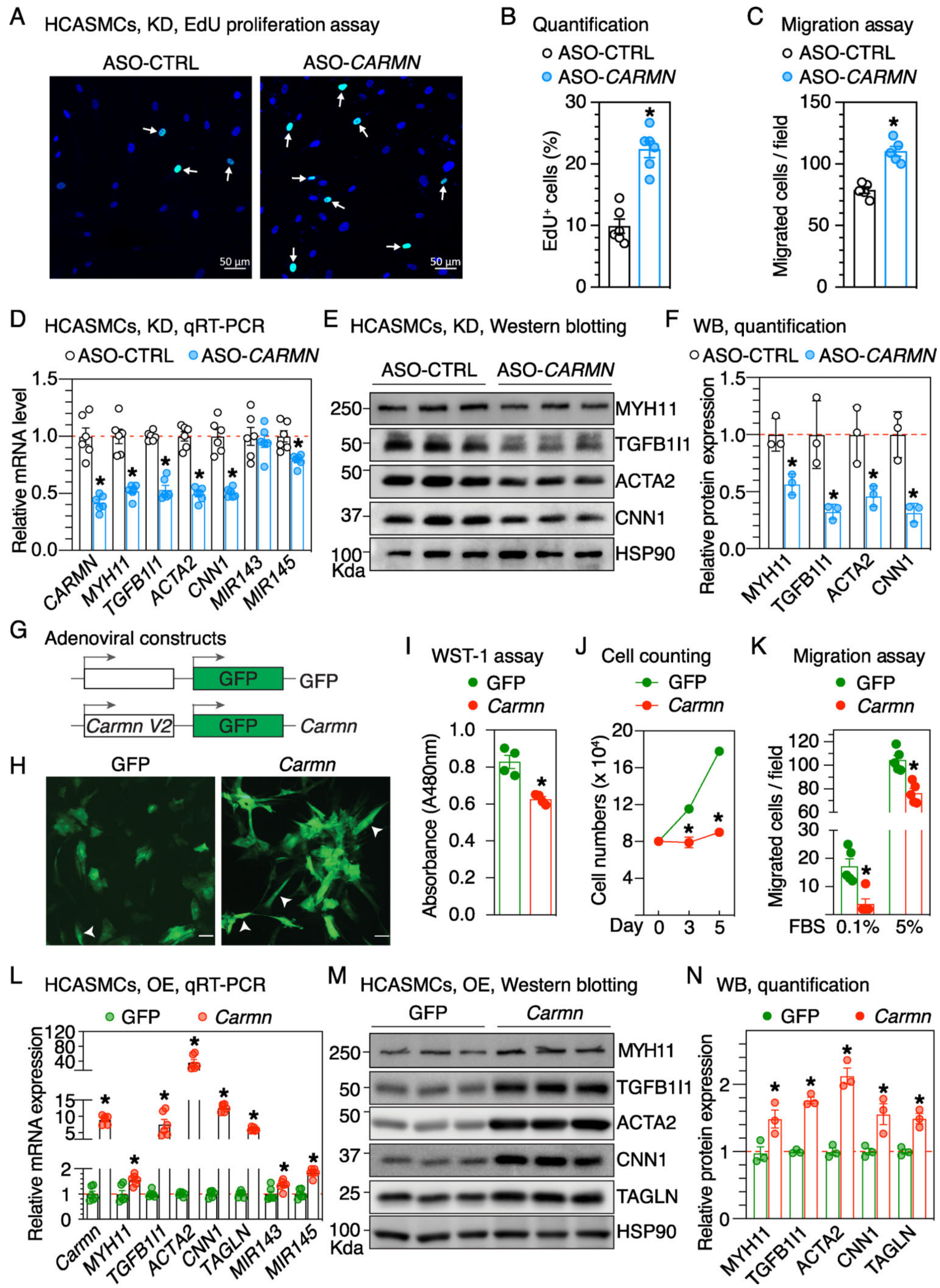

Figure 5. *CARMN* is required for maintaining the VSMC contractile phenotype in vitro.

(**A**) *CARMN* or control phosphorothioate-modified antisense oligonucleotide (ASO) (ASO-CTRL) were transduced into human coronary artery SMCs (HCASMCs) for 5 days to knock down (KD) endogenous *CARMN* expression. EdU incorporation assays were performed to assess cell proliferation following depletion of *CARMN* in HCASMCs. Arrows point to the representative EdU positive cells. (**B**) Quantitative analysis of EdU positive cells following *CARMN* depletion. N=6; *P < 0.05; unpaired Student's t-test. (**C**) Boyden chamber assays were performed to examine cell migration after knocking down *CARMN* in HCASMCs.

N=5; *P < 0.05; unpaired Student's t-test. (**D**) Expression of SM-contractile genes and *MIR143/145* was analyzed by qRT-PCR or (**E**) Western blot. (**F**) Densitometric analysis of protein expression as shown by Western blot (WB) in "**E**" with normalization to the loading control HSP90. Relative signal in ASO-CTRL group was set to 1. N=3; *P < 0.05; unpaired Student's t-test. (**G**) *Carmn* or control GFP adenovirus were generated and (**H**) transduced into HCASMCs for 48 hours. An increased number of spindle shaped cells (arrowheads) was observed in *Carmn* over-expressed HCASMCs. Scale bar: 50 μm. (**I**) Cell proliferation was measured by cell proliferation WST-1 kit and (**J**) cell number counting at the indicated time points. N=4 for WST-1 assay and N=3 for cell counting assay; *P < 0.05; unpaired Student's t-test for WST-1 assay; two-way ANOVA followed with a post-hoc testing within day for cell counting assay. (**K**) Over-expression of *Carmn* attenuated the migration of HCASMCs cultured in the medium containing 0.1% or 5% FBS as revealed by Boyden chamber assays. N=5; *P < 0.05; unpaired Student's t-test. (**L**) Expression of SM-contractile genes and *MIR143/145* was analyzed by qRT-PCR or (**M**) Western blot after over-expressing *Carmn* for 48 hours. (**N**) Densitometric analysis of protein levels as shown in "**M**". N=3; *P < 0.05; unpaired Student's t-test.

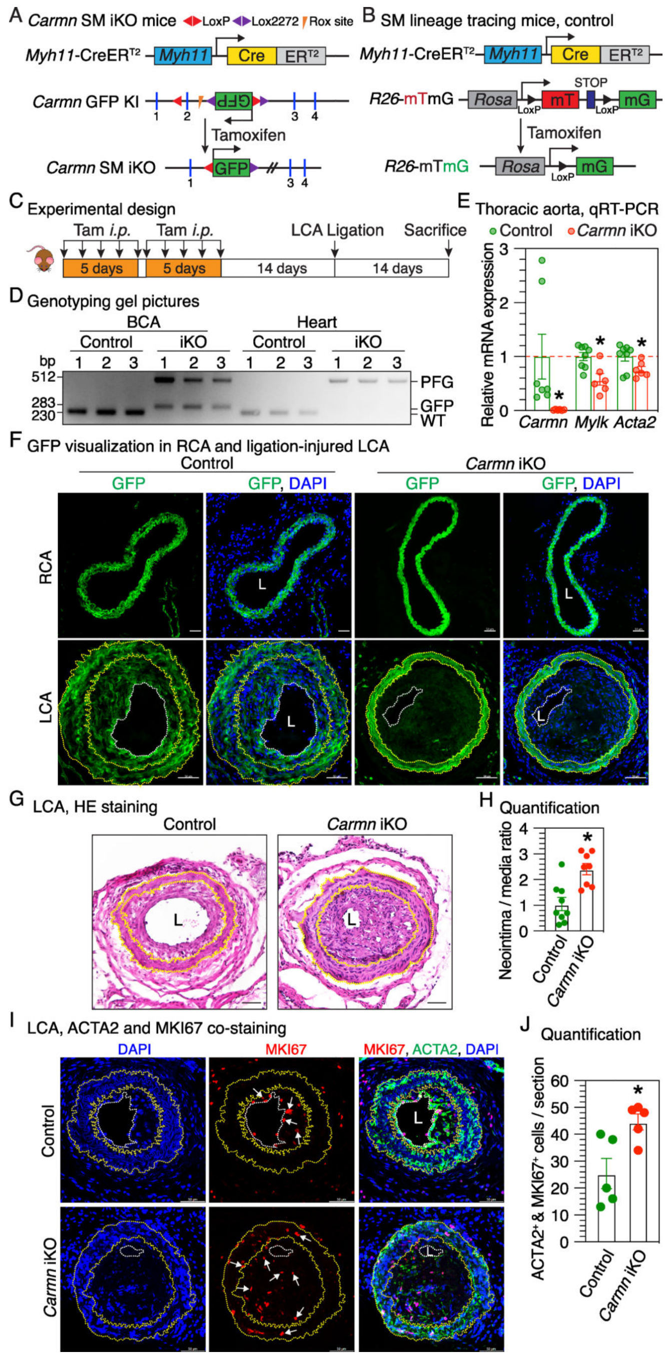

Figure 6. SM-specific deletion of *CARMN* exacerbates injury-induced neointima formation in mice.

(A) Strategy for generating SM-specific *Carmn* inducible KO (iKO) mice and **(B)** *Carmn*$^{W/W}$; *Myh11*-CreER^{T2}; mTmG$^{+/-}$ SM lineage tracing control mice. **(C)** Experimental design: tamoxifen (Tam) was injected intraperitoneally (*i.p.*) to both control and SM-specific *Carmn* iKO mice (8-week-old, male mice only) for 10 days (2 days' break after the first 5 injections) to activate Cre recombinase. Two weeks after the last injection, left carotid artery (LCA) ligation was performed with the uninjured right carotid artery (RCA) serving as the contralateral control. Both LCA and RCA were harvested 14 days post-injury to assess neointima formation. **(D)** Representative agarose gel picture of PCR genotyping using DNA extracted from brachiocephalic artery (BCA) or heart as templates. **(E)** qRT-PCR analysis of *Carmn* and SMC contractile gene expression in thoracic aorta of control or SM-specific *Carmn* iKO mice. N=6–8; *P < 0.05; unpaired Student's t-test. **(F)** Direct visualization of GFP (green) in normal RCA and ligation-injured LCA of SM lineage tracing control mice or SM-specific *Carmn* iKO mice. Nuclei were counterstained with DAPI (blue). Yellow and white dashed lines denote external/internal elastic lamina and neointima border, respectively. L: lumen. Scale bar: 50 μm. **(G)** Representative pictures of HE staining in ligation-injured LCA of control or SM-specific *Carmn* iKO mice. Yellow dashed lines denote external/internal elastic lamina. L: lumen; Scale bar: 100 μm. **(H)** Quantification of neointima/medial layer ratio of injured LCA. N=8–9; *P < 0.05; unpaired Student's t-test. **(I)** IF staining of MKI67 (red) and ACTA2 (green) in ligation-injured LCA of control or SM-specific *Carmn* iKO mice. Nuclei were counterstained with DAPI (blue). Scale bar: 20 μm. **(J)** Quantification of numbers of ACTA2 and MKI67 double positive cells (white arrows) in medial and neointimal areas of ligation-injured LCA in both control and SM-specific *Carmn* iKO mice. L: lumen; N=5; *P < 0.05; unpaired Student's t-test.

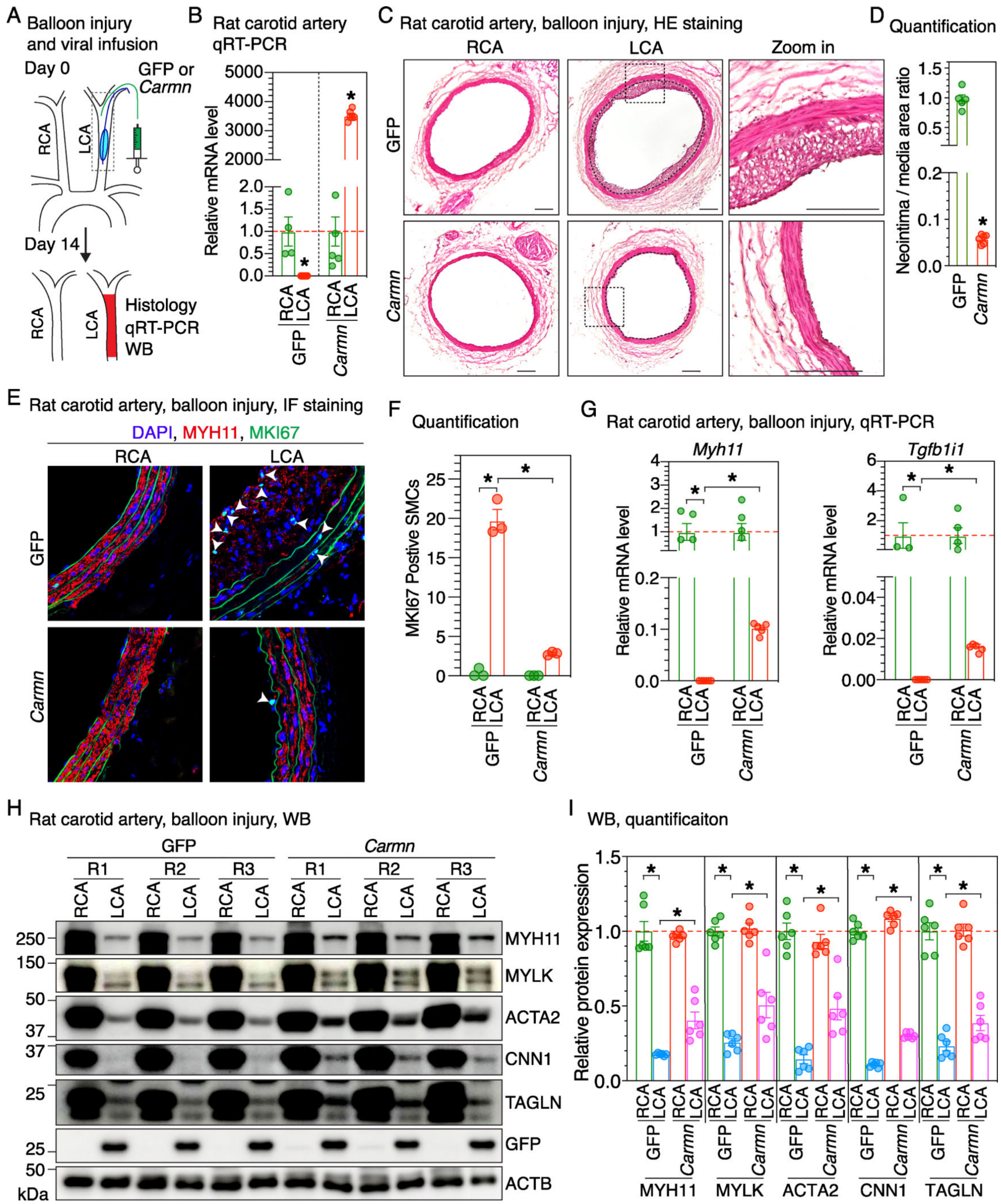

Figure 7. Restoration of *Carmn* expression attenuates neointima formation in rat carotid artery balloon injury model.

(A) Schematic diagram of the experimental design. Adenoviruses expressing GFP or *Carmn* were infused into balloon-injured left carotid artery (LCA) after injury. Fourteen days post injury, intact right carotid artery (RCA) and injured LCA were harvested for histology, qRT-PCR or Western blotting analysis. **(B)** qRT-PCR analysis of *Carmn* expression in rat control RCA or balloon-injured LCA infused with either GFP or *Carmn* adenovirus. Endogenous rat *Carmn* expression in RCA and LCA of GFP adenovirus-infected rats was measured with the primers specific for rat *Carmn*. Both RCA and LCA of rats that were locally delivered with mouse *Carmn* adenovirus were measured with the primers specific for mouse *Carmn*. N=4–5; *P < 0.05; unpaired Student's t-test. **(C)** HE staining of carotid artery sections from either control RCA or balloon-injured LCA that were transduced with GFP or *Carmn* adenovirus. M: media; NI: neointima; Scale bar: 100 μm (**D**) Quantification of neointima/media layer ratio of LCA sections shown in "**C**". N=6; *P < 0.05; unpaired Student's t-test. **(E)** Co-staining of proliferative marker MKI67 (green) and SM-specific marker MYH11 (red) was performed in the rat control RCA or balloon-injured LCA that was infused with either GFP or *Carmn* adenovirus. Nuclei were counterstained with DAPI (blue). Arrowheads point to representative MKI67 positive SMCs. Scale bar: 50 μm. **(F)** Quantification of MKI67 positive SMCs shown in "**E**". N=3; *P < 0.05; two-way repeated measures ANOVA. (**G**) qRT-PCR analysis of *Myh11* and *Tgfb1i1* expression in rat control RCA or balloon-injured LCA that was infused with either GFP or *Carmn* adenovirus. N=4; *P < 0.05; two-way repeated measures ANOVA. (**H**) Western blotting analysis of SM-specific contractile proteins in rat (R) control RCA or balloon-injured LCA with either GFP or *Carmn* adenoviral transduction. **(I)** Densitometric analysis of protein expression as shown in "**H**". Signal of control RCA from the rat transduced with GFP adenovirus group was set to 1. N=6; *P < 0.05; two-way repeated measures ANOVA.

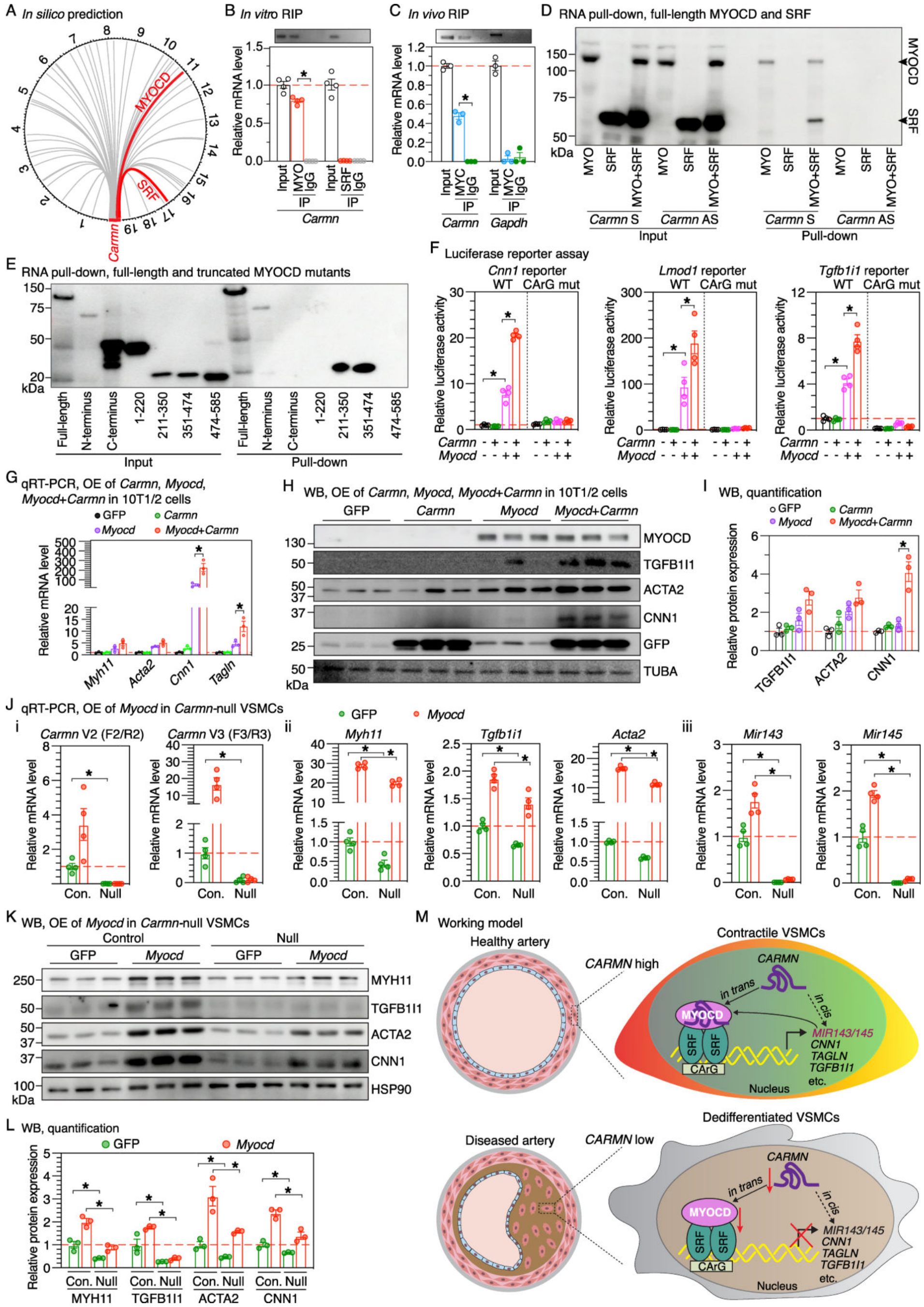

Figure 8. *CARMN* directly binds to MYOCD to enhance MYOCD function.

(A) Circos plot showing 55 genes that encode proteins predicted to interact with *Carmn*. The outer rings indicate chromosome numbers. The grey lines indicate predicted *Carmn*-interacted protein genes that are aligned to their chromosome locations, with SRF and MYOCD in red. **(B)** *In vitro* RIP to examine the direct interaction between *Carmn* and bacterially expressed MYOCD (MYO) or SRF. qPCR was performed to measure the relative *Carmn* binding to MYOCD or SRF using primers designed for *Carmn*. Samples immunoprecipitated with IgG served as control. The upper gel picture represents pooled

PCR products from each group. N=4; *P < 0.05; unpaired Student's t-test. **(C)** RIP assay was performed using lysates extracted from aortic tissues of MYC/HA-tagged *Myocd* mouse with anti-MYC antibody. qPCR was performed to examine relative binding between MYOCD and *Carmn* or *Gapdh* that served as a negative control. Samples immunoprecipitated with IgG served as additional control. The upper gel picture represents pooled PCR products from each group. N=3; *P < 0.05; unpaired Student's t-test. **(D)** RNA pull-down assay was performed using biotinylated sense (S) *Carmn* and bacterially expressed full-length of MYOCD (MYO) and SRF, followed by Western blotting. Pull-down assays performed with biotinylated antisense (AS) *Carmn* served as negative control. **(E)** RNA pull-down assay was performed using biotinylated *Carmn* sense probe and bacterially expressed full-length or truncated MYOCD mutants to map the interaction regions of MYOCD with *Carmn*. **(F)** Luciferase reporter assays were performed to examine the effects of *Carmn* on MYOCD-induced promoter luciferase activity of wildtype (WT) or CArG box mutated SM-specific genes *Cnn1*, *Lmod1*, and *Tgfb1i1*. N=4; *P < 0.05; two-way ANOVA. **(G)** qRT-PCR and **(H)** Western blotting analysis showing *Carmn* enhances MYOCD-induced SM-specific gene expression in 10T1/2 fibroblast cells. **(I)** Densitometric analysis of protein expression as shown in "**H**". N=3; *P < 0.05; two-way ANOVA. **(J)** VSMCs isolated from the aortae of $Carmn^{PFG/PFG}$ mice were infected with Cre adenovirus to delete *Carmn in vitro* (*Carmn*-null). Cells infected with LacZ adenovirus served as control (Con.). Cells were then infected with either GFP or *Myocd* adenovirus and harvested for qRT-PCR or **(K)** Western blotting analysis of SM-specific genes. F2/R2 and F3/R3 represent primers specifically detecting *Carmn* transcript V2 and V3, respectively. N=4; *P < 0.05; two-way ANOVA (**J**). **(L)** Densitometric analysis of protein expression as shown in "**K**". N=3; *P < 0.05; two-way ANOVA. **(M)** Proposed working model for *CARMN* function in maintaining contractile phenotype of VSMCs. SMC nucleus-restricted lncRNA *CARMN* acts *in-trans* by directly binding to MYOCD (solid arrow), which promotes MYOCD/SRF transcriptional activity to induce expression of CArG box-dependent SM-specific genes such as *MIR143/145*, *CNN1*, *TAGLN* and *TGFB1I1*, leading to a contractile phenotype of VSMCs in healthy artery. It is not clear whether *in cis*-mechanism contributes to the regulation of *MIR143/145* expression by *CARMN* in VSMCs (dashed arrow). Conversely, in response to stimuli of SMC phenotypic modulation in diseased artery, *CARMN* expression is down-regulated, leading to diminished transcriptional activity of MYOCD/SRF complex. As a result, expression of SM-specific genes is attenuated, thereby driving SMC into dedifferentiation phenotype.